Thank you to both reviewers for their helpful comments. We have responded to all reviewer comments.

Other changes in addition to changes from the responses to reviewers:

Author institution updated for Edward J. Dlugokencky to "National Oceanic and Atmospheric Administration, Global Monitoring Laboratory, Boulder, CO, USA"

NOAA ESRL aircraft changed to "NOAA GML aircraft network" due to an updated name for this program.

The format of this response is alternating paragraphs of: reviewer comment, response, reviewer comment, response...

Response to reviewer 1. The ordering of the responses are: major comments from reviewer 1, minor comments from reviewer 1.

Responses to Major comments from Reviewer 1:

Reviewer 1: 1-1) 3. MUSES-AIRS Optimal Estimation of CH4 from single-footprint, original (non cloud- cleared) AIRS radiances:, page 5, "Good quality and sensitivity flagging for AIRS CH4:" 1-1) The authors should give more explanations on the quality flags which they have applied to AIRS CH4 data. Are "radiance residual rms and mean" for all wavelength regions used in the AIRS CH4 retrieval? What are "NESR", "|KdotdL|", and "TSUR"? These terms may be referred to in some previous papers describing AIRS CH4 retrieval algorithm, but the authors should at least spell them out and give their definition.

Response: A description of the quality flags was updated and a references given that defines and describes each quality flag. Text added to the paper, "Quality flags are discussed in more detail in the Aura-TES user's guide (pp 27-30, Herman et al., 2018). The specific flags used for AIRS CH4 are as follows, which were set by minimizing the standard deviation of small clusters of retrievals and to standardize the sensitivity:"

Reviewer 1: 1-2) "Cloud OD < 0.3" means that clouds that partially exist in the AIRS FOVs probably affect the AIRS retrievals and the amount of the effects would vary depending on the cloud OD itself. How did the authors evaluate the effects in this research?

Response: A plot of error versus cloud optical depth was added to the supplement. Text added, "* Cloud optical depth < 0.3. This ensures that the cloud is not opaque and there is fairly uniform sensitivity so that the bias correction is fairly consistent. The bias versus cloud optical depth is shown in the supplement."

Reviewer 1: 1-3) How did the authors define tropopause height at each CH4 measurement location and calculate its tropospheric and stratospheric degrees of freedom? 1-4)

Response: The tropopause height was obtained from GMAO files. Text added to the paper after Eq. 2: "The degrees of freedom, DOFs, describing the sensitivity of x to the true state, and is equal to the trace of A_xx. The degrees of freedom in the troposphere is equal to the trace of the averaging kernel corresponding to the troposphere, and the degrees of freedom in the stratosphere is equal to the trace of the averaging kernel corresponding to the stratosphere. The troposphere is defined using the tropopause height parameter from version 5 of the NASA Global Modeling and Assimilation Office (GMAO) Goddard Earth Observing System (GEOS-5) model (Molad et al., 2012)."

Reviewer 1: 1-4) What is "predicted error"? The authors discuss the "predicted error" in the later part of the text, but they should here mention the definition.

Formatted: Normal

Formatted: Font color: Black

Formatted: Normal, Border: Top: (No border), Bottom: (No border), Left: (No border), Right: (No border), Between : (No border), Tab stops: 3.13", Centered + 6.27", Right

Response: The predicted error is the total error from the linear estimate, Eq. 4, and is a field in the output product. Text added to the paper after Eq. 7 "The square root of 7b is the predicted observation error.", and text added to the description of Fig. 3, "Figure 3 shows the predicted errors for the AIRS partial column XCH4 VMR within the pressure levels measured by the aircraft. The measurement error (light green) is 18 ppb (from the last term of Eq. 7b) , and the total error for a single observation (including smoothing error) is 41 ppb. A component of the total error, the cross-state error, is estimated as 21 ppb (from Eq. 7b)."

Reviewer 1: 2) 3.1 Retrieval Error Characteristics, page 6, Equation (2) The authors should briefly explain the definition of A_xy. In this case, x indicates a methane profile and y does simultaneous retrieved parameters such as temperature and there is no relationship (cross-term) in nature between methane and temperature.

Responses: Added in new text after Eq. 2 "Axx describes the dependence of x on the true state x, and Axy describes the dependence of x on the true state y, which is non-zero because of correlations in the Jacobians, K, for x and y."

Reviewer 1: 3) "3.2 Approach for Comparing AIRS measurements to aircraft profiles", page 7, Equation (4) In my understanding, A_cc is a symmetric matrix with a dimension of the number of atmospheric layers that can be observed by aircraft, while A matrix has a dimension of the number of full atmospheric layers from the surface to the top of the atmosphere. A_cs should be a non-square matrix, and how is it defined by the cross-terms of the A matrix? More explanation should be needed for readers.

Response: Added in new text after Eq. 4 "So, if for example, the aircraft measured pressures 0-9, and did not measure pressure levels 10-65, then Acc=A[0:9,0:9] and Acs=A[0:9,10:65], where A is the full averaging kernel."

Reviewer 1 4) "3.2 Approach for Comparing AIRS measurements to aircraft profiles", page 8, Equation (6) Sa matrix should in principle includes random errors only. The first term A_cb Sbb_a A_cb(T) comes from radiance biases that should have systematic characteristics. The other three terms or the second and the last terms only may be randomly distributed errors. Is it possible to treat errors that may have different characteristics in the same manner?

Response: Equation 6, as the reviewer notes, only addressed random errors. Added Equation 6a, which is the bias component of error, and Equation 6b, the current Equation 6, the variable component of the error. Added additional text to describe this. "Equation 6a represents the propagation of mean biases from: (1) fixed (non-retrieved) parameters, e.g. spectroscopy (b), (2) jointly retrieved parameters, e.g. temperature, (y), (3) "stratospheric", describing the impact of the part of the atmosphere not covered by the aircraft on the measured part (xs), or (4) measurement errors (n) into biases of xc. The mean bias from 6a is difficult to characterize theoretically and is characterized during validation, and assumed to be primarily from the first term (e.g. spectroscopy). Equation 6b represents the propagation of these same error types into a varying error. Although Eq. 6b has overall zero bias, it can produce regional and temporal biases, e.g. as seen in Connor et al. (2016), where these biases approach zero over long enough spatial or temporal scales. The error covariances all represent fractional errors, in log(VMR). The error in ppb is approximately the fractional error times the methane value in ppb."

Reviewer 1, 5): "3.2 Approach for Comparing AIRS measurements to aircraft profiles", page 9, lines 259-260 It should be more explained why "red" (mean obs. errors) minus "green" yields the cross-state error.

Response: We removed the statement in question. It now reads, "Figure 3 shows the predicted errors for the AIRS partial column XCH4 VMR within the pressure levels measured by the aircraft. The measurement error (light green) is 18 ppb (from the last term of Eq. 7b) , and the total error for a single observation (including smoothing error) is 41 ppb. A component of the total error, the cross-state error, is estimated as 21 ppb (from Eq. 7b)."

Reviewer 1 6) "3.3 Estimating validation error due to aircraft not measuring the stratosphere", page 9 I agree that the assumption in the stratosphere could significantly contribute to the differences between AIRS and aircraft data, but the amount of the validation error attributed to the stratosphere where aircraft cannot make observations should depend on how

Formatted: Normal

Formatted: Font color: Black

Formatted: Normal, Border: Top: (No border), Bottom: (No border), Left: (No border), Right: (No border), Between : (No border), Tab stops: 3.13", Centered + 6.27", Right

accurate each of the models (a priori, LMDz, and GC) can define the tropopause height; this may be a reason why we see relatively larger variabilities in the differences between AIRS and aircraft (simulated) in northern mid-latitudes."

Response: We agree that the stratospheric error depends on the accuracy of the model used to extend the validation data. We estimated the error for the model that we used in our validation. Added statement on page 9 "This estimate depends on the accuracy of the model used to extend the aircraft profile during the validation process, and was estimated for the model that we used in validation."

Reviewer 1 7) Overall, it is better to describe a bit more clearly which of errors the authors think is a systematic or random one. The authors have already referred to which is which for each of the error components in several parts of the text, but there are too many error values and they sometimes resemble another one; it is an option to add a table to summarize the characteristics of each of the error components.

Response: Added statement after Eq. 6b to indicate that the overall bias primarly results from the first term in Eq. 6a. However, the split of errors into "random" and "systematic" is not straightforward. Added a statement after Eq. 6b, "Although Eq. 6b has overall zero bias, it can produce regional and temporal biases, e.g. as seen in Connor et al. (2016), where these biases approach zero over long enough spatial or temporal scales."

Minor comments from reviewer 1.

1) Figure 1 It is easy to see if the international dateline is centered.

Response: Referee suggests switching view on Figure 1. This was updated, as well as the colors and symbols used, as requested elsewhere.

2) page 5, line 137 "... such as check on the " "2, residual signals, ...", a symbol before "2" is missing.

Response: Fixed. "We use similar quality flags as the TES retrievals such as checks on the radiance residual, ..."

3) page 6, line 165 The symbols in the text do not correspond to those in the equations.

Response: Fixed.

4) Figure 2 The authors should explain the color shading in more details; which pressure layers do colors indicate?

Response: The levels are listed in the figure caption with several of the pressures shown on the plot itself.

5) page 8, line 251 Which is correct, A_cn in the text or A_cs in Equation (6)? Or A_cs and A_cs are used as the same meaning?

Response: The reviewer helpfully pointed out inconsistent notation. We did a switch from calling the non-measured part of the atmosphere "n" to "s" during the paper formation, so all the Acn should be Acs. Updated the text. Thank you.

6) Figure 3 The authors should give more explanations in the caption using the terms in the equations in the text.

Response: We now show the equation for the "smoothing error" in Eq. 5. Label Eq. 7 as the "observation error". The text for Figure 3 now reads, "The total error shown is the smoothing error (Eq. 5) plus the observation error (Eq. 7b). The measurement error is the last term of Eq. 7b, and the only fully random error."

7) "Figures 5 and 6 it may be better to replace the figure numbers".

Formatted: Normal

Formatted: Font color: Black

Formatted: Normal, Border: Top: (No border), Bottom: (No border), Left: (No border), Right: (No border), Between : (No border), Tab stops: 3.13", Centered + 6.27", Right

Response: I switched these two figures (was a clearer note in embedded comments in paper)

8) page 10, lines 294-295 Why did the author choose HIPPO-4 observations to estimate bias correction values?

Response: Added a sentence to describe why HIPPO-4 was chosen, "HIPPO-4 was selected as it covers a wide range of latitudes and so that the bias correction can be set and tested with two independent datasets."

9) page 10, lines 295-296 Equation 5 is split into two: Eq. 5a and Eq. 5b. Are they combined?

Response: Yes, Eq. 5 was split into 5a and 5b, but later referred to as "Equation 5". The text was updated here and one other place to refer to Eq. 5b.

10) Figures 6 and 7 The bias values shown in the figures do not correspond to the values in the text. The authors should explain the values in the captions of the figures.

Response: Thank you for noticing that. New text is added for Fig. 5 and 7 (Fig 5 & 6 were swapped based on the previous reviewer comments). The values in the paper were outdated, and updated. Here is the updated text describing the biases shown in Fig 7, "Figure 7 shows the same comparisons as Fig. 5 after bias correction (described in Section 3.4). The mean bias is 1 ppb, and the RMS difference is 24 ppb. The overall land bias is 12 ppb, and the overall ocean bias is -2 ppb. The bias calculated in Fig. 7 is weighs every point equally. Table A.1 shows a slightly different result for these biases, where the bias is calculated by campaign, then averaged over all campaigns. In Table A.1 the partial column XCH4 VMR within the pressure levels measured by the aircraft has a bias of 16 ppb for land, and -2 ppb for ocean."

11) page 12, line 350 Where does "24" come from?

Response: This comes from the single observation RMS, shown in Fig. 7. The text is updated to "Figure 8 shows the predicted error, assuming that the error is random, which is calculated by dividing the single observation error (24 ppb RMS shown in Fig. 7) by the square root of the number of observations that are averaged. The mean predicted error for the averaged data, assuming random errors, is 6 ppb. The actual standard deviation between the averaged AIRS and HIPPO or ATom data is ~17 ppb, which is much larger and indicates that the errors within 1 day and 50 km are correlated."

12) page 12, line 363 It is better to add an explanation of 5.4 ppb (growth rate per year calculated at this site?).

Response: Added text "The growth rate of 5.4 ppb/year is the mean increase during the AIRS record time period (2002-2019) estimated from the NOAA Global Monitoring Laboratory global surface measurements (https://esrl.noaa.gov/gmd/ccgg/trends_ch4/). Since we are converting matched pairs of aircraft and AIRS to 2012, the differences between these matched pairs is unaffected by the accuracy of the conversion to 2012."

13) page 12, lines 378-380 Does this sentence mean that there are some correlations among each of the differences between collocated AIRS and aircraft pairs and the correlations cannot be compensated when taking averages on a daily basis?

Response: Yes. Updated the wording to say this more clearly, "The standard deviation for daily observations is 15.2 ppb. This can be compared to the predicted error assuming randomness of 5.9 ppb (23 ppb divided by the square root of the number of observations averaged) Since 15.2 ppb is much larger than 5.9 ppb, this indicates that there are correlated (non-random) errors on the order of 15 ppb when averaging nearby observations within 1 day."

The format of this response is alternating paragraphs of: reviewer comment, response, reviewer comment, response... The ordering of the responses are: major comments from reviewer 2 and minor comments from reviewer 2 (comments taken from the embedded PDF).

Formatted: Normal

Formatted: Font color: Black

Formatted: Normal, Border: Top: (No border), Bottom: (No border), Left: (No border), Right: (No border), Between : (No border), Tab stops: 3.13", Centered + 6.27", Right

Reviewer 2 major comments:

Reviewer 2: (1) During first reading I got confused at several instances because an error was introduced by number, while the path towards derivation of this error was only explained in the next para or section. I always thought I have missed a part of the manuscript but found out with re-reading that the explanation follows on the number. It would be easier (at least for readers like me) to first provide the explanation and then the number.

Response: A reference to the section where each is calculated was added, or the "preview" was removed. "Figure 3 shows the predicted errors for the AIRS partial column XCH4 VMR within the pressure levels measured by the aircraft. The measurement error (light green) is 18 ppb (from the last term of Eq. 7b) , and the total error for a single observation (including smoothing error) is 41 ppb. A component of the total error, the cross-state error, is estimated as 21 ppb (from Eq. 7b)." The smoothing error estimate now shown after the new Eq. 5 and the text states that this is calculated from Eq. 5.

Reviewer 2: (2) The authors use very often the term "partial column". They need to introduce how the partial methane column over the pressure range the aircraft had measured has been calculated, both for the aircraft and AIRS data (what shape of the methane profile? where do pressure and temperature profiles come from?); further, the figures usually show volume mixing ratios (in ppb) instead of partial colums. This might sound picky, but I think this accurateness in wording should be kept.

Response: At the beginning of Section 2, 2 sentences were added to describe how partial columns are created, "The retrieval estimates AIRS CH4 dry volume mixing ratio (VMR) profile. When a "partial column quantity" is validated, the retrieved CH4 profile is post-processed into partial column XCH4 VMR relative to dry air, with methodology from Connor et al. (2008) and Kulawik et al. (2017), where the VMR's at the pressure levels are weighted according to a pressure weighting function, resulting in a partial column volume mixing ratio (VMR).". Based on reviewer 2's comments here and elsewhere, the paper was previously not clear that the partial column quantity is XCH4 VMR. The wording was updated throughout the paper to indicate that the validated quantity was "the AIRS partial column XCH4 VMR within the pressure levels measured by the aircraft"

Reviewer 2 (3): I was a bit surprised that the two models that were used to assess the so-called "validation error" (i.e. the unknown stratospheric part of the profile) provided largely different results (4.4 vs. 15.7 ppb). I think the authors should elaborate a little more on the reasons for this large difference. This is particularly important because the averaging kernels in Fig. 2 demonstrates that the stratospheric information is large mapped into the troposphere below 300 hPa, i.e. the AIRS signal obviously depends a lot on the assumptions about the stratosphere. Is it possible that the use of other models leads to even larger estimates of the validation error?

Response: Added additional text and reference on the errors from model extension of the aircraft profile: "The methane profile has a strong, spatially varying negative vertical gradient in the stratosphere. Models in general have a positive bias in the extratropical stratosphere (Patra et al., 2011). In GEOS-Chem 4x5, the column bias is shown in Figure 2c of Turner et al. (2015) and further discussed in Maasakkers (2019), which resolves the bias to the stratosphere, and model stratospheric accuracy is an active research area (Ostler et al., 2016; Maasakkers et al., 2019)."

Reviewer 2 (4) A side remark without relevance to the revision of this paper: the SPARC TUNER activity has worked on recommendations about error reporting. A paper on this topic has just been accepted by AMT. It would be nice to look into that paper (amt-2019-350) and possibly following these recommendations in future.

Response: Thank you for this information It is good to standardize validation.

Embedded notes/comments from Referee 2. I summarized the comments and wrote the response.

Formatted: Normal

Formatted: Font color: Black

Formatted: Normal, Border: Top: (No border), Bottom: (No border), Left: (No border), Right: (No border), Between : (No border), Tab stops: 3.13", Centered + 6.27", Right

1) Abstract: Define "validation error" Response: Update wording in abstract, and also change name to "validation uncertainty" "We estimate a 16 ppb validation uncertainty because the aircraft typically did not measure methane at altitudes where the AIRS measurements have some sensitivity, e.g. the stratosphere, and there is uncertainty in the truth that we validate against."

Section 2: Question about how the partial column is defined and the profile shape assumptions. The text was updated in response to this and to an earlier comment to clarify that a profile is retrieved, and then an XCH4 VMR is calculated. "The retrieval estimates AIRS CH4 dry volume mixing ratio (VMR) profile. When a "partial column quantity" is validated, the retrieved CH4 profile is post-processed into partial column XCH4 VMR relative to dry air, with methodology from Connor et al. (2008) and Kulawik et al. (2017), where the VMR's at the pressure levels are weighted according to a pressure weighting function, resulting in a partial column volume mixing ratio (VMR)."

3) cm-1 formatting. Response: Updated.

4) removed URL from citation as suggested by reviewer.

5) Request figure 1: center legend on Pacific. Update symbols. Remove gray color. Label aircraft sites. Response: Updated as requested

6) Description of Sa is needed. Response: Updated section around the new Equation 5, "The expected total error includes the smoothing error, which the covariance of the hcAccxc-x ac (Rodgers, 2000), where the covariance of xc-x ac is the a priori covariance, Saxx. The smoothing error is: (Eq 5) We estimate the smoothing error for the partial column XCH4 VMR within the pressure levels measured by the aircraft to be 30 ppb, using Eq. 5. This estimate strongly depends on Saxx, the a priori covariance, which is the same as in Worden et al. (2012); briefly 5% diagonal variability with correlations in pressure set from the MOZART model."

7) Description of the selection of quality flags. "The specific flags used for AIRS CH4 are as follows, which were set by minimizing the standard deviation of small clusters of retrievals and to standardize the sensitivity:"

8) The reviewer suggests that things like "|KdotdL| < 0.23 should be given proper names. Response: Since these variables are not referred to outside of this section, and additionally are referencing an existing data user's guide, the updates were to the description of the equation, e.g. |KdotdL| < 0.23 --> The absoluate value of KdotdL < 0.23.

Equation 1, question about "G" versus "Gr". Response: Removed the R. Thanks.

Question about "sum over i" in Equation 1. Response: change b to a vector and the summation is implied just like all the other matrix multiplication.

Comment on A = dx/dx "Careful with log! Response: Yes, thank you, the equations are mixing up x and log(x). The intention was that x=log(VMR), so A = dx/dx, and K = dradiance/dx = dradiance/d(log(VMR)). Other issues fixed in this section from the reviewer.

Reviewer: Comment on estimate of smoothing error. Response: Addressed above, the smoothing error was estimated from the new Eq. 5.

Reviewer at Eq. 5b, "It is necessary to mention that this step is possible because the levels of the aircraft measurement are assumed uncorrelated." Response: This is now Eq. 6a, and the text was updated, "Equation 6a accounts for all of the AIRS smoothing error, whereas Equation 6b (the equation used in this work, other than Section 3.3) only accounts for the smoothing error from the part of the atmosphere measured by the aircraft profile. [...] The difference from Eqs. 6a and 6b is discussed in Section 3.3. "

Formatted: Normal

Formatted: Font color: Black

Formatted: Normal, Border: Top: (No border), Bottom: (No border), Left: (No border), Right: (No border), Between : (No border), Tab stops: 3.13", Centered + 6.27", Right

Eq 6, "This step comes as surprise. Including 1-2 steps or explanation would be helpful." Response: Added new Eq. 5, introducing the a priori covariance, Eq. 7a, introducing the bias, and Eq. 7b, the covariance of 7a. Updated wording, "Equation 7a is the predicted bias between x_c (the measured AIRS value) and x_aircraft_c (the aircraft value with the AIRS Averaging kernel applied), and is the expected difference of Eqs. 4 and 6b. Equation 7b is the covariance of Eq. 7a, and estimates the predicted error."

Equation 6, "Acb is not defined". Response: change Acb to GcKb.

Line 235, "Here the explanation should be given that this is because the retrieval vector is log(VMR)." Response: updated. "Because the retrieved quantity log(VMR), the error in ppb is approximately the fractional error times the methane value in ppb."

Line 255, "Define validation error". Response: Now it is consistently called "validation uncertainty" throughout the paper rather than "validation error" and "validation uncertainty".

Line 259, "Where do these errors come from?". Response: These errors are now tied to equations.

Line 266, The reviewer notes that not only the stratosphere influences the troposphere, but the troposphere influences the stratosphere, due to the broad sensitivity. Response: Added sentence, "Similarly, the true state in the troposphere influences retrieved values in the stratosphere."

Line 282. Is the 16 ppb the larger of the two errors from model propagation? Response: We updated this to set the "validation uncertainty" to the average of the two model results, 10 ppb. This agrees with the previous result from Wunch et al. (2010).

Reviewer comment: How does the profile extension relate to the "validation uncertainty"? Doesn't it relate more to the bias estimate? Response: The profile extension obviously affects the bias versus validation data which affects the bias correction. However, it is most relevant to the uncertainty that results from extending the aircraft profile using a model. Text update, "Appendix A shows further analysis of mean differences of AIRS minus aircraft for different profile extension choices. The bias varies by ~ 5 ppb for different profile extension choices when comparing at 700 hPa, ~10 ppb for different profile extension choices when comparing at 500 hPa, and ~11 ppb for different profile extension choices when comparing the column above 750 hPa."

Line 291. Reviewer requests that Worden et al., 2011 bias correction be summarized briefly. Response: Added text, "We therefore use the bias correction approach described in Worden et al. (2011), where a bias profile (which varies by pressure) is passed through the averaging kernel to account for the AIRS sensitivity, as seen in Eq. 8. The form of the bias profile, delta_bias set by Eq. 9."

Eq 7. Reviewer wonders if A is a vector. Response: A is a matrix, as x-hat is a profile, as shown in Fig. 6. Text updated, "Where x = ln(VMR), because the retrieved quantity is ln(VMR), delta_bias is a vector, and A is the averaging kernel matrix for x = ln(VMR)"

Eq 7. Reviewer wonders about the handling of log. Response: text and equations updated to handle log consistently.

Line 315. Reviewer wonders why there is a bias peak about 200 hPa. Response: It seems that the bias is increasing through the stratosphere, whereas the sensitivity is decreasing above 100 hPa, and these two combine to generate a peak about 200 hPa. But this is speculation.

Formatted: Normal

Formatted: Font color: Black

Formatted: Normal, Border: Top: (No border), Bottom: (No border), Left: (No border), Right: (No border), Between : (No border), Tab stops: 3.13", Centered + 6.27", Right

Section 4 title changed from "Evaluation against aircraft data by latitude" to "Evaluation against aircraft data versus latitude", because as the reviewer points out, there is no fitting of bias or skill as a function of latitude.

Line 319 Reviewer suggests wording update to, "Figure 6 shows a comparison between all AIRS measurements within 50 km and 9h of an aircraft measurement over the pressure range of the partial column measured by the aircraft.". Response: The wording was updated to, "Figure 5 [figure numbering update] shows a comparison between all AIRS measurements within 50 km and 9h of an aircraft measurement and the aircraft. The quantity compared is the partial column XCH4 VMR within the pressure levels measured by the aircraft."

Figure 7 legend unreadable. Response: Add text in the figure caption with the information in the legend.

Line 334-335, reviewer questions what the legend means, e.g. 0.0 +/- 4. Response: This was not well explained in the text previously. This is an estimate of the overall bias and uncertainty in the bias. Each campaign or station's bias is independently calculated and then the mean and standard deviation are calculated. A new sub-section was added at the end of Section 4.1, "4.2.6 The bias and bias uncertainty The bias is estimated by calculating the mean bias for each campaign or station separately, then calculating the mean and standard deviation for all campaigns / stations. The bias versus HIPPO is 0 ± 4 ppb. The bias versus ATom is 3 ± 4 ppb. The bias versus NOAA measurements is 9 ± 7 ppb."

Reviewer wants "roughly the same location and time" defined in line 344. Response: Text added to clarify, "The bias component is approximately the same for all AIRS methane measurements taken on the same day within 50 km, as we do not expect large variations in temperature and water vapor errors over these scales, which we presume to be a driver of these correlated errors."

Reviewer says this sentence is hard to parse, "The number of AIRS observations averaged ranges from 9 to 53 and averages 20.". Response: This was updated to, "We average over 1 day, the AIRS observations matching a single HIPPO or ATom measurement, within +-50 km and 9 hours of the measurement. We specify that there needs to be at least 9 AIRS observations for each comparison so that the systematic error, and not the precision (or measurement error), is the dominant term. These daily AIRS averages contain, on average, 20 AIRS observations."

In Figure 9, the reviewer noted that the figure showed VMR but was indicated as a partial column. Response: This is an XCH4 partial column, as noted above and now explained in the paper.` The wording describing the partial column throughout the paper, to remove this confusion, is, "The partial column XCH4 VMR within the pressure levels measured by the aircraft".

365-375. The reviewer says that this section is hard to follow and needs explanation on the importance of the values shown. Response: Updated this text to indicate what the numbers mean, and what the findings are. Also separate into 4 new subsections, discussing daily, monthly, 3-month, and seasonal cycle averaging. Added a new section on the bias characterization (in response to a previous comment.

The rewritten text is (the next 7 paragraphs):

"4.2.1 Daily average errors at TGC We look at daily averages versus aircraft data, and find a similar result as found with comparisons to Atom and HIPPO: daily averages have much larger errors than would be predicted if random errors are assumed. The standard deviation of (AIRS minus aircraft) at TGC is 24 ppb, the standard deviation for (daily AIRS average minus aircraft) is 11.5 ppb, as seen in Fig. 9a, and the predicted error for daily averages, assuming randomness in the error, is 6.0 ppb. Therefore, similarly to ATom and HIPPO, errors within 1 day and 50 km contain 11.5 ppb correlated error.

"4.2.2 Monthly average errors at TGC The aircraft measurements are usually taken about twice per month. The standard deviation of (monthly AIRS average minus aircraft) is 8.2 ppb (Figure 9b) for months containing more than 1 aircraft

Formatted: Normal

Formatted: Font color: Black

Formatted: Normal, Border: Top: (No border), Bottom: (No border), Left: (No border), Right: (No border), Between : (No border), Tab stops: 3.13", Centered + 6.27", Right

observation. This is compared to the daily error divided by the square root of the number of days averaged, 8.0 ppb. Therefore, errors for observations ~2 weeks apart are uncorrelated.

"4.2.3 3-month average errors at TGC We average over 3-month scales, where averages must have at least 3 days. The standard deviation of (3-month AIRS average minus aircraft) is 6.2 ppb. The predicted error, taking the 11.5 ppb daily error and dividing by the square root of the number of days averaged, is 6.0 ppb. Therefore, errors for 3-month averages are ~uncorrelated.

"4.2.3 Seasonal cycle average errors at TGC We average matched pairs within each month from any year. (AIRS minus aircraft) for these averages, have a standard deviation of 5.9 ppb, whereas the predicted error, from the daily average divided by the square root of number of observations, is 4.2 ppb.

"4.2.4 Summary of average errors at TGC To summarize, averaging AIRS observations within one day reduces the error versus aircraft, but correlated errors prevent daily averaged errors from dropping below 11.5 ppb. Averaging daily averages over 1 or 3 months equals the daily error divided by the square root of the number of days averaged, indicating that errors are random in this domain. However, averaging months from multiple years, does not reduce the error below 6 ppb, either due to correlated errors, or validation uncertainty.

"4.2.5 Summary of errors at all NOAA aircraft sites Table A.3 in Appendix A shows the single-observation standard deviation for all NOAA aircraft sites. The ocean vs. land observations show similar values, with land and ocean standard deviations within 2 ppb. A single land observation has a standard deviation versus aircraft observations of 23 ppb for the partial column XCH4 VMR within the pressure levels measured from the aircraft, in agreement with predicted observation error of 23 ppb. The standard deviation for daily averages is 15.2 ppb. This can be compared to the predicted error for the daily averages, assuming randomness, of 5.9 ppb. This indicates that there are correlated (non-random) errors on the order of 15 ppb when averaging observations within 50 km and 1 day. The monthly standard deviation is 10.9, in reasonable agreement with the predicted of 9.4 ppb (from the daily average standard deviation divided by the number of observations averaged). The seasonal cycle average, which is a monthly average of all matched pairs from all years, has a standard deviation of 7.7 ppb, which is similar to the predicted error of 6.9 ppb (from the daily average divided by the square root of number of observations). We find that estimating the error as the daily standard deviation divided by the square root of the number of days averaged is a reasonable estimate of the actual error.

"4.2.6 The bias and bias uncertainty The bias is estimated by calculating the mean bias for each campaign or station separately, then calculating the mean and standard deviation for all campaigns / stations. The bias versus HIPPO is 0 ± 4 ppb. The bias versus ATom is 3 ± 4 ppb. The bias versus NOAA measurements is 9 ± 7 ppb."

Formatted: Normal

Formatted: Font color: Black

Formatted: Normal, Border: Top: (No border), Bottom: (No border), Left: (No border), Right: (No border), Between : (No border), Tab stops: 3.13", Centered + 6.27", Right

Evaluation of single-footprint AIRS CH_4 Profile Retrieval Uncertainties Using Aircraft Profile Measurements

Susan S. Kulawik[1], John R. Worden[2], Vivienne H. Payne[2], Dejian Fu[2], Steve C. Wofsy[3], Kathryn McKain[4,5], Colm Sweeney[4], Bruce C. Daube, Jr[6], Alan Lipton[7], Igor Polonsky[7], Yuguang He[7], Karen E. Cady-Pereira[7], Edward J. ~~Dlugokencky[8]~~Dlugokencky[4], Daniel J. Jacob[6], Yi ~~Yin[8]~~Yin[8]

[1]BAER Institute, 625 2nd Street, Suite 209, Petaluma, CA, USA
[2]Jet Propulsion Laboratory, California Institute of Technology, Pasadena, CA, USA
[3]School of Engineering and Applied Sciences and Department of Earth and Planetary Sciences, Harvard University, Cambridge, MA 02138, USA
[4]National Oceanic and Atmospheric Administration, ~~Earth System Research~~Global Monitoring Laboratory, Boulder, CO, USA
[5]University of Colorado, Cooperative Institute for Research in Environmental Sciences, Boulder, CO, USA
[6]Harvard University, Cambridge, MA 02138, USA
[7]Atmospheric and Environmental Research, Inc., Lexington, Massachusetts, USA

~~[8]NOAA ESRL Global Monitoring Division, Boulder, Colorado~~
~~[9]California~~[8]Division of Geological and Planetary Sciences, California Institute of Technology, Pasadena, CA, USA

Correspondence to: Susan S. Kulawik (susan.s.kulawik@nasa.gov)

Abstract.

We evaluate the uncertainties of methane optimal estimation retrievals from single footprint thermal infrared observations from the Atmospheric Infrared Sounder (AIRS). These retrievals are primarily sensitive to atmospheric methane in the mid-troposphere through the lower stratosphere (~2 to ~17 km). We compare to in situ observations made from aircraft during the Hiaper Pole to Pole Observations (HIPPO~~), the NASA~~) and Atmospheric Tomography Mission (ATom) campaigns, and from the NOAA ~~ESRL~~GML aircraft network, between the surface and 5-13 km, across a range of years, latitudes between 60 S to 80 N, and over land and ocean. After a global, pressure dependent bias correction, we find that the land and ocean have similar biases and that the reported observation error (combined measurement and interference errors) of ~27 ppb is consistent with the standard deviation between aircraft and individual AIRS observations. A single ~~measurement~~observation has measurement (noise related) uncertainty of ~17 ppb, a ~20 ppb uncertainty from radiative interferences (e.g. from water, temperature, etc.), and ~ 30 ppb due to "smoothing error", which is partially removed when making comparisons to in situ measurements or models in a way that account for this regularization. We estimate a ~~16~~10 ppb validation ~~error~~uncertainty because the aircraft typically did not measure methane at altitudes where the AIRS measurements have some sensitivity, e.g. the stratosphere~~.~~, and there is uncertainty in the truth that we validate against. Daily ~~averaged AIRS measurements of at least 9 observations over spatio-temporal domains of < 1 degree and 1 hour have a standard deviation of ~17 ppb versus~~ averaging only partly reduces the difference between aircraft and satellite observation, likely because ~~the observation~~of correlated errors introduced into the retrieval from temperature and water vapor ~~(for~~. For example~~) are only partly reduced through~~, averaging 9 observations only

Formatted: Normal

Formatted: Font color: Black

Formatted: Font color: Black

Formatted: Font color: Black

Formatted: Font color: Black

Formatted: Normal, Border: Top: (No border), Bottom: (No border), Left: (No border), Right: (No border), Between : (No border)

Formatted: Font color: Black

Formatted: Font color: Black

Formatted: Font color: Black

Formatted: Normal, Border: Top: (No border), Bottom: (No border), Left: (No border), Right: (No border), Between : (No border), Tab stops: 3.13", Centered + 6.27", Right

reduces the aircraft/model difference to ~17 ppb versus the expected ~10 ppb. Seasonal averages can reduce this ~17 ppb uncertainty further to ~10 ppb, as determined through comparison with NOAA aircraft, likely because uncertainties related to radiative effects of temperature and water vapor ~~can be~~are reduced when averaged over a season.

1 Introduction

Advances in remote sensing, global transport modeling, and an increasingly dense network of surface measurements have led to substantive advances in evaluating the components and error structure of the global methane budget and the processes controlling this budget. For example, Frankenberg et al. (2005, 2011) showed that total column methane estimates could be derived from near infrared (NIR) radiances at ~1.6 microns measured by the Scanning Imaging Absorption Spectrometer for Atmospheric Cartography (SCIAMACHY). Since then, methane retrievals have also been applied to NIR radiances from the Greenhouse Gases Observing Satellite (GOSAT) instrument (e.g. Parker et al., 2011; Schepers et al., 2012), launched in 2009 ~~with measurements~~, and the ~~TROPOspheric~~TROPOspheric Monitoring Instrument (TROPOMI, e.g. Hu et al., 2018), launched in 2017. These data have sufficient accuracy to map regional surface methane enhancements (e.g. Kort et al., 2014; Wecht et al., 2014) and point source anomalies (Varon et al., 2019; Pandey et al., 2019). Estimates of the free-tropospheric methane concentrations from spaceborne measurements in the thermal infrared (TIR) at ~8 microns were demonstrated using radiances from the Aura Tropospheric Emission Spectrometer (TES, Worden et al., 2012; 2013b), the Atmospheric Infrared Sounder (AIRS, e.g. Xiong et al., 2013), the Infrared Atmospheric Sounding Interferometers (IASI, e.g. Ravazi et al., 2009; De Wachter et al., 2017; Siddans et al., 2017), the Cross-Track Infrared Sounders (CrIS, e.g. Smith and Barnet, 2019) and TIR GOSAT measurements (de Lange and Landgraf, 2018). TIR methane measurements have been used to evaluate the role of fires (e.g. Worden et al., 2013b; 2017a), Asian emissions and stratospheric intrusions (e.g. Xiong et al., 2009; 2013) on the global methane budget.

The goal of this paper is to evaluate the uncertainties of new methane retrievals from AIRS single footprint, original (non-cloud-cleared) radiances using aircraft measurements from the HIAPER Pole-to-Pole Observations (HIPPO) and Atmospheric Tomography Mission (ATom) campaigns and National Oceanic and Atmospheric Administration (NOAA) ~~Earth System Research~~Global Monitoring Laboratory (~~ESRL~~GML) aircraft network, taken between 2006 and 2017. Evaluation of these uncertainties are needed to determine if AIRS methane data can characterize and improve errors in global chemistry transport models. For example, a recent paper by Zhang et al. (2018) combined synthetic CrIS and TROPOMI methane retrievals and a global inversion system to show that it would be possible to infer the north-south gradient of OH, the primary methane sink, to within 10%, and temporal variations of OH concentrations. However, knowing the accuracy of the methane data is important for inferring the uncertainty in the spatio-temporal variability of OH. Over decadal time scales, OH can vary by 3-5% (e.g. Turner et al., 2018a, 2018b, 2019; Rigby et al., 2017). Therefore, to be useful for understanding OH, monthly or seasonally averaged AIRS data should have an uncertainty that is less than 3-5% (55-99 ppb).

Formatted: Normal

Formatted: Font color: Black

Formatted: Normal, Border: Top: (No border), Bottom: (No border), Left: (No border), Right: (No border), Between : (No border), Tab stops: 3.13", Centered + 6.27", Right

In this paper we present an evaluation of methane retrievals derived from AIRS single footprint radiances. We follow an optimal estimation approach (Rodgers, 2000), based on the heritage of the Aura Tropospheric Emission Spectrometer (TES) algorithm (Bowman et al., 2006), now called the MUlti-SpEctra, MUlti-SpEcies, MUlti-Sensors (MUSES) algorithm (Worden et al., 2006, 2013b; Fu et al., 2013, 2016, 2018, 2019). The MUSES algorithm uses radiances from one or multiple instruments to quantify and characterize geophysical parameters derivable from those radiances. The optimal estimation method provides the vertical sensitivity (i.e., the averaging kernel matrix) and estimates of the uncertainties due to noise and to radiative interferences such as temperature, N2O, and water vapor. We compare AIRS retrievals with corresponding aircraft data over a range of latitudes and longitudes in order to evaluate the calculated uncertainties over ocean and land. Much of the description of the forward model and retrieval approach is provided in Worden et al. (2012, 2019). We therefore refer the reader to these papers for a more in-depth description of the retrieval approach and only summarize aspects here that are relevant for comparing the AIRS methane retrievals to aircraft data.

2 Datasets used in this paper

The quantities of interest that we validate in this paper are a) the AIRS CH_4 dry volume mixing ratio (VMR) at particular pressure values between 750 hPa and 300 hPa, or b) the AIRS CH_4 dry VMR partial column XCH_4 covering the same pressure range that is measured by the aircraft. We use aircraft profiles which span the pressure range that contains at least 0.20 degrees of freedom for the AIRS CH_4 partial column. The retrieval estimates AIRS CH_4 dry volume mixing ratio (VMR) profile. When a "partial column quantity" is validated, the retrieved CH_4 profile is post-processed into partial column XCH_4 VMR relative to dry air, with methodology from Connor et al. (2008) and Kulawik et al. (2017), where the VMR's at the pressure levels are weighted according to a pressure weighting function, resulting in a partial column volume mixing ratio (VMR).

2.1 Description of AIRS

The AIRS instrument is a nadir-viewing, scanning infrared spectrometer (Aumann et al., 2003; Pagano et al., 2003; Irion et al., 2018; DeSouza-Machado et al., 2018) that is onboard the NASA Aqua satellite and was launched in 2002. AIRS measures the thermal radiance between approximately 3-12 microns with a resolving power of approximately 1200. For the 8 micron spectral range used for the $HDO/H_2O/CH_4$ retrievals, the spectral resolution is ~1 wavenumber (cm^{-1}), with a gridding of ~0.5 cm^{-1}, and the signal-to-noise (SNR) ranges from ~400 to ~1000 over the 8 micron region for a typical tropical scene. A single footprint has a diameter of ~15 km in the nadir; given the ~1250 km swath, the AIRS instrument can measure nearly the whole globe in a single day. The Aqua satellite is part of the "A-Train" that consists of multiple satellites and instruments, including TES, in a sun-synchronous orbit at 705 km with an approximately 1:30 am and 1:30 pm equator crossing-time. In this paper, we use only daytime data to match the validation observations.

Formatted: Normal

Formatted: Superscript

Formatted: Superscript

Formatted: Font color: Black

Formatted: Normal, Border: Top: (No border), Bottom: (No border), Left: (No border), Right: (No border), Between : (No border), Tab stops: 3.13", Centered + 6.27", Right

~~1~~2.2 Overview of Aircraft Data

Measurements from the HIPPO (Wofsy et al., 2012) and ATom (Wofsy et al., 2018) aircraft campaigns ~~(Wofsy et al., 2012)~~ provide ~~an~~ excellent ~~data set~~datasets for satellite validation, due to ~~the~~their wide latitudinal coverage, the large vertical extent of the profiles (up to 9-12 km), and the availability of campaigns over a wide range of months. Each of the five HIPPO campaigns flew south, then north over a period of weeks, often using a different path for the northern and southern legs, with campaign dates in 2009 - 2011. Atmospheric methane concentrations were measured with a quantum cascade laser spectrometer (QCLS) at 1 Hz frequency with accuracy of 1.0 ppb and precision of 0.5 ppb (Santoni et al., 2014). HIPPO methane data are reported on the WMO X2004 scale and have been used in several other studies to evaluate satellite retrievals of methane (e.g. Alvarado et al., 2015; Wecht et al., 2012; Crevoisier et al., 2013). Comparisons with NOAA flask data showed a mean positive bias of 0.85 ppb for the QCLS during the HIPPO campaigns, which is consistent with the estimated QCLS accuracy of 1.0 ppb (Santoni et al., 2014; Kort et al., 2011). We used 396 QCLS CH_4 profiles from the HIPPO campaigns. Using coincidence criteria of ±9 hours, ±50 km, 22,271 AIRS observations were processed, of which 5537 passed quality flags. The latitude of the matches ranges from 57S to 81N.

We compare AIRS to observations from the ATom aircraft campaigns 1-4 (Wofsy et al., 2018). This comparison provides ~~validatation~~validation ~7 years after HIPPO, between 2016 and 2018. Similar to HIPPO, these observations include observations in the Pacific Ocean, but ATom also includes observations in the Atlantic (as seen in Table A.1 and Fig. 1). ATom methane data are reported on the WMO X2004A scale. We used 289 profiles from the ATom campaigns from the NOAA Picarro instrument (Karion et al., 2013). For more information on the instrument, see https://espo.nasa.gov/sites/default/files/archive_docs/NOAA-Picarro_ATom1234_readme.pdf. Using coincidence criteria of ±9 hours, ±50 km, 21,225 AIRS observations were processed, of which 4913 passed quality flags. The latitude of the matches ranges from 65S to 65N.

The NOAA ~~ESRL~~GML aircraft network observations (Cooperative Global Atmospheric Data Integration Project, 2019) are taken twice per month at fixed sites primarily in North America, and also Rarotonga (RTA) at 21S (Sweeney et al., 2015~~, http://dx.doi.org/10.1002/2014JD022591).~~). NOAA aircraft network methane data are reported on the WMO X2004A scale. Although HIPPO data are not reported on the same scale as ATom and NOAA aircraft network data, differences in values of calibration tanks used for HIPPO (Santoni et al., 2014) on the two different scales are < 1 ppb. We match AIRS and NOAA aircraft observations between 2006 and 2017, with coincidence criteria of 50 km~~,~~ and 9 hours, finding ~43,000 matches, and 18,000 good quality matches following the retrieval, to 719 aircraft measurements, at sites ACG (67.7N, 164.6E, 401 matches), ESP (49.4N, 126.5E, 2743 matches), NHA (43.0N, 70.6E, 2682 matches), THD (41.1N, 124.2E, 1551 matches), CMA (38.8N, 74.3E, 3269 matches), TGC (27.7N, 96.9E, 1944 matches), and RTA (21.2S, 159.8E, 810 matches).

Formatted: Normal

Formatted: Font color: Black

Formatted: Normal, Border: Top: (No border), Bottom: (No border), Left: (No border), Right: (No border), Between : (No border), Tab stops: 3.13", Centered + 6.27", Right

Figure 1 shows the locations of all the aircraft data used for the comparisons described in this paper. Most of the ocean measurements are from the HIPPO and ATom campaigns that spans a range of latitudes, whereas most of the land measurements are taken over North America~~..~~

3 MUSES-AIRS Optimal Estimation of CH_4 from single-footprint, original (non-cloud-cleared) AIRS radiances

Worden et al. (2012, 2019) describe in detail the forward model and retrieval approach used for estimating methane from TES and AIRS radiances. The radiative transfer forward model used for this work is the Optimal Spectral Sampling (OSS) fast radiative transfer model (RTM) (Moncet et al., 2005, 2008, 2015). In particular, radiances from the thermal infrared bands at 8 and 12 microns are used to quantify profiles of atmospheric concentrations of CH_4, HDO, H_2O, N_2O, as well as temperature, emissivity, and cloud properties. The atmospheric parameters are retrieved as vertical profiles. Since we use optimal estimation, or OE, ~~(~~e.g. Rodgers, 2000; Bowman et al., 2006) to estimate these quantities we can characterize the vertical resolution and uncertainties of these retrievals, which allows us to ~~c~~ompare them to models and independent data sets, while accounting for the regularization used for the retrieval. We follow the OE approach for the Aura TES instrument (e.g. Bowman et al., 2006; Worden et al., 2006, 2012) but with some differences. First, methane retrievals using the TES radiances are obtained using only the 8 micron band, because of slight calibration differences between the detectors that measure the 12 and 8 micron bands (e.g. Shephard et al., 2008; Connor et al., 2011). For the AIRS retrievals, we use both the 8 and 12 micron bands in order to better constrain temperature in the troposphere and stratosphere. Secondly, the TES based retrieval uses the ratio of a jointly-retrieved N2O profile to the CH_4 profile in order to help correct biases related to temperature variations in the (UTLS) upper-troposphere lower-stratosphere (Worden et al., 2012). However, the N_2O correction is not used for the AIRS retrievals because we can jointly estimate temperature in the UTLS region using the 12 micron band. We use similar quality flags as the TES retrievals such as checks on the ~~□2~~radiance residual, residual signal, and cloud optical depth as discussed in Kulawik et al. (2006a, 2006b), except that we screen out cloudy and low-sensitivity cases, resulting in about 1/4 of the data passing screening. Quality flags are discussed in more detail in the Aura-TES user's guide (pp 27-30, Herman et al., 2018). The specific flags used for AIRS CH_4 are as follows, which were set by minimizing the standard deviation of small clusters of retrievals and to standardize the sensitivity:

Good quality and sensitivity flagging for AIRS CH_4:

- Radiance residual rms < 1.5. This ~~screens off~~parameter is the ~~standard deviation of the radiance residual (the~~mean difference between the observed and fit radiance normalized by the ~~NESR).~~radiance measurement error.
- ~~|~~The absolute value of Radiance residual mean~~|~~ < 0.15. This parameter screens off the mean difference of the radiance residual.

Formatted: Normal

Formatted: Subscript

Formatted: Outline numbered + Level: 1 + Numbering Style: Bullet + Aligned at: 0.75" + Indent at: 1"

Formatted: Font color: Black

Formatted: Normal, Border: Top: (No border), Bottom: (No border), Left: (No border), Right: (No border), Between : (No border), Tab stops: 3.13", Centered + 6.27", Right

- ~~|~~The absolute value of KdotdL~~|~~ < 0.23. This ~~screens off the~~ parameter is the mean difference of the dot product of the Jacobians and the radiance residual ~~and indicates~~normalized by the radiance measurement error, and smaller values indicate that there is little remaining information ~~relative to the noise level about the surface and atmosphere~~ in the ~~retrieval~~signal.
- ~~TSUR <~~ The surface temperature minus the near-surface atmospheric temperature value ~~+~~< 30K. This ensures that the thermal gradient is less than 30K between the surface and lowest atmospheric temperature.
- Cloudtop pressure > 90 hPa. This ensures that the retrieved cloudtop ~~is not above 90 hPa~~pressure is in or near the Troposphere.
- Cloud ~~OD~~optical depth < 0.3. This ensures that the cloud is not opaque and there is fairly uniform sensitivity ~~below the~~so that the bias correction is fairly consistent. The bias versus cloud optical depth is shown in the supplement.
- Cloud variability versus wavenumber < 1.5 * cloud OD. This ensures that the cloud optical depth does not vary too much ~~with wavenumber~~over the retrieval window.
- Degrees of freedom > 1.1~~.~~, defined following Eq. 2. This ensures a minimum sensitivity so that the bias correction is fairly consistent.
- Tropospheric degrees of freedom > 0.7~~.~~, defined following Eq. 2. This ensures a ~~minimum~~consistent Tropospheric sensitivity~~.~~, so that the bias correction is fairly consistent.
- Stratospheric degrees of freedom < 0.5~~.~~, defined following Eq. 2. This ensures that there is ~~not too much~~a consistent stratospheric sensitivity ~~in the stratosphere~~, so that the bias correction is fairly consistent.
- Predicted error on the column above 750 hPa < 53 ppb. The predicted error is the total error from the linear estimate, Eq. 7b, and is included in the output product. This ensures that the predicted error, which is correlated to the actual error, is not too large.

3.1 Retrieval Error Characteristics

Detailed descriptions of the use of optimal estimation (OE) to infer trace gas profiles from remote sensing radiance measurements retrieval is included in numerous publications (e.g. Rodgers, 2000; Worden et al., 2006; Bowman et al., 2006). However, we present a partial description here as it is relevant for comparing the AIRS methane retrievals and aircraft profile measurements. As discussed in Rodgers (2000), the estimate for a trace gas profile inferred (or inverted) from a radiance spectrum is described by the following linear equation:

~~$\hat{\mathbf{x}} = \bar{x_a} + \mathbf{A}(\mathbf{x} - \bar{x_a}) + \mathbf{G_k} \sum_i \bar{\mathbf{K}_i^b} (\mathbf{b}_i - \mathbf{b}_i^a) + \mathbf{Gn}$ (1)~~

$$\hat{x} = x_a + A(x - x_a) + G\ K^b b_{error} + Gn \quad (1)$$

Formatted: Normal

Formatted: Font: Times New Roman

Formatted: Font color: Black

Formatted: Normal, Border: Top: (No border), Bottom: (No border), Left: (No border), Right: (No border), Between : (No border), Tab stops: 3.13", Centered + 6.27", Right

where ~~x^~~ $\hat{x}$ is the estimate of Log(VMR), ~~⟦x_ ⟧ a^~~ x_a is the log of the a priori concentration profile used to regularize the inversion, G is the gain matrix, $\boldsymbol{b}_{error}$ represents errors in systematic parameters, with K^b the sensitivity of the radiance to changes in **b**. We split x into [x,y], where x is the quantity of interest, the methane profile, and y are the jointly estimated quantities (such as temperature, water vapor, clouds, and surface properties), which results in the cross-state error (Worden et al., 2004; Connor et al., 2008).

~~$\hat{\mathbf{x}} = \mathbf{x_a} + \mathbf{A_{xx}}(\mathbf{x} - \mathbf{x_a}) + \mathbf{G_K}\sum_i \mathbf{K_i^b}(\mathbf{b_i} - \mathbf{b_i^a}) + \mathbf{A_{xy}}(\mathbf{y} - \mathbf{y_a}) + \mathbf{Gn}$ (2)~~ $\hat{x} = x_a + A_{xx}(x - x_a) + G\ K^b b_{error} + A_{xy}(y - y_a) + Gn$ **(2)**

For the AIRS (and TES) OE methane retrievals, $\mathbf{x_a}$ comes from the MOZART atmosphere chemistry model (e.g. Brasseur *et al*., 1998). The vector **x** is the "true state", or in this case the (log) concentration profile. The matrix **A** is the averaging kernel matrix or ~~**A =** $\frac{\partial \hat{x}}{\partial x}$~~ $A = \frac{\partial \hat{x}}{\partial x}$ and describes the vertical sensitivity of the measurement. A_{xx} describes the dependence of $\hat{x}$ on the true state x, and A_{xy} describes the dependence of $\hat{x}$ on the true state y, which is non-zero because of correlations in the Jacobians, **K**, for x and y. The matrix **G** relates changes in the radiance (**L**) to perturbations in **x**, ~~**G =** $\frac{\partial x \partial L}{\partial L \partial x}$~~ $G = \frac{\partial x}{\partial L}$. The vector **n** is the noise vector, the matrix **K** is the sensitivity of the radiance to changes in (log) concentration ~~**K =** $\frac{\partial L}{\partial log(x)} = \frac{\partial L}{\partial log(VMR)}$~~ $K = \frac{\partial L}{\partial x} = \frac{\partial L}{\partial log(VMR)}$, and the set of vectors $\mathbf{b}_i$ represent interference errors not estimated from the observed radiances. The true state, noise vector, and interference errors as described here are the "true" values and are therefore not actually known but are represented in this form so that we can calculate how their uncertainties affect the estimate ~~x^~~ $\hat{x}$. An example averaging kernel matrix is shown in Figure 2 and shows that AIRS based estimates of methane are most sensitive to methane in the free-troposphere and lower-stratosphere as demonstrated previously for AIRS and other TIR based estimates of tropospheric methane (e.g. Xiong *et al*., 2016; de Lange and Landgraf, 2018).

The degrees of freedom, DOFs, describing the sensitivity of $\hat{x}$ to the true state, and is equal to the trace of A_{xx}. The degrees of freedom in the troposphere is equal to the trace of the averaging kernel corresponding to the troposphere, and the degrees of freedom in the stratosphere is equal to the trace of the averaging kernel corresponding to the stratosphere. The troposphere is defined using the tropopause height parameter from version 5 of the NASA Global Modeling and Assimilation Office (GMAO) Goddard Earth Observing System (GEOS-5) model (Molad et al., 2012).

Finally, we look at the quantity of interest, $\hat{x}$ = **hx.** The vector **h** combines all the necessary operations that maps the (log) concentration profiles to whatever quantity is needed such as selecting one particular pressure level (e.g. **h**= [0,0,0,1,0,0,0, …],

Formatted: Normal

Formatted: Font: Times New Roman

Formatted: Font: Times New Roman

Formatted: Font: Cambria Math

Formatted: Font: Times New Roman

Formatted: Font: Times New Roman

Formatted: Font: Times New Roman

Formatted: Font: Times New Roman

Formatted: Font: Times New Roman

Formatted: Font: Times New Roman

Formatted: Font: Times New Roman

Formatted: Font: Times New Roman

Formatted: Font: Times New Roman

Formatted: Font color: Black

Formatted: Normal, Border: Top: (No border), Bottom: (No border), Left: (No border), Right: (No border), Between : (No border), Tab stops: 3.13", Centered + 6.27", Right

selecting a column average, (**h** = pressure weighting function) – see Connor et al., 2008 or Kulawik et al., 2017) or selecting the VMR mean (e.g. **h**=[:]=1/m, where m is the number of pressure levels to average).

$$\hat{x} = \sout{\mathbf{h}\hat{\mathbf{x}}}\ h\hat{x} \qquad (3a)$$

~~$\hat{x} = \mathbf{h}\mathbf{x}_a + \mathbf{h}\mathbf{A}_{xx}(\mathbf{x}-\mathbf{x}_a) + \mathbf{h}\mathbf{G}_x\sum_i \mathbf{K}_i^b(\mathbf{b}_i-\mathbf{b}_i^a) + \mathbf{h}\mathbf{A}_{xy}(\mathbf{y}-\mathbf{y}_a) + \mathbf{h}\mathbf{G}\mathbf{n}$ (3b)~~

$$\hat{x} = hx_a + hA_{xx}(x-x_a) + hG_x K^b b_{error} + hA_{xy}(y-y_a) + hG_x n \qquad (3b)$$

In Eq. 3a, the vector ~~$\hat{\mathbf{x}}$~~ $\hat{x}$ (denoted in bold) is converted to the scalar of interest, $\hat{x}$ (non-bold, italic). In our validation comparisons, **h** is used to select 1) a specific pressure level that is measured by the aircraft, 2) the partial column ~~average over~~ XCH_4 VMR within the pressure levels measured by the aircraft, and 3) the partial column ~~above~~ XCH_4 between 750 hPa and the top of the atmosphere.

3.2 Approach for Comparing AIRS measurements to aircraft profiles

A challenge in comparing the satellite-based AIRS measurements to aircraft data is that the aircraft will typically measure only a section of the atmosphere (e.g. the troposphere), whereas the AIRS measurements are sensitive, to varying degrees (see Fig. 2), to the entire atmosphere. To account for these differences, we divide the atmosphere into two parts $\mathbf{x} = [\mathbf{x}_c,\mathbf{x}_s]$: where $\mathbf{x}_c$ is the part measured by the aircraft (denoted **c** for airCraft), and $\mathbf{x}_s$ is the part not measured by the aircraft (denoted **s** for Stratospheric):

~~$\hat{x}_c = \mathbf{h}_c\mathbf{x}_a + \mathbf{h}_c\mathbf{A}_{cc}(\mathbf{x}_c - x_a^c) + \mathbf{h}\mathbf{G}_x\sum_i \mathbf{K}_i^b(\mathbf{b}_i-\mathbf{b}_i^a) + \mathbf{h}_c\mathbf{A}_{cy}(\mathbf{y}-\mathbf{y}_a) + \mathbf{h}_c\mathbf{A}_{cs}(\mathbf{x}_s - x_a^s)A_{cs}(\mathbf{x}_s - x_a^s) + \mathbf{h}_c\mathbf{G}\mathbf{n}$ (4)~~

$$\hat{x}_c = h_c x_a + h_c A_{cc}(x_c - x_a^c) + hG_c K^b b_{error} + h_c A_{cy}(y-y_a) + h_c A_{cs}(x_s - x_a^s)A_{cs}(x_s - x_a^s) + h_c G_c n \qquad (4)$$

where the term $\mathbf{A}_{cs}$ is the cross-term in the averaging kernel that describes the partial derivatives of the aircraft-measured levels (e.g. the troposphere) to the un-measured levels (e.g. the stratosphere). Equation 4 describes how the AIRS measurement ~~$\hat{x}_c$~~ $\hat{x}_c$ responds to the true state $[\mathbf{x}_c,\mathbf{x}_s]$. So, if for example, the aircraft measured indices [0:9], and did not measure pressure levels [10:*], then $A_{cc} = A[0{:}9, 0{:}9]$ and $A_{cs} = A[0{:}9, 10{:}65]$, where A is the full averaging kernel.

We compare our AIRS observation, ~~$\hat{x}_c$~~ $\hat{x}_c$ in Eq. 4, to our aircraft observation, ~~$x_{aircraft}$~~ $x_{aircraft}$. To compare directly to the aircraft observation (without accounting for AIRS sensitivity) we would compare to ~~$\hat{x}^c_{aircraft} = \mathbf{h}_c x_{aircraft}$. However, the~~ $\hat{x}^c_{aircraft} = h_c x_{aircraft}$. The expected total error ~~would include~~ includes the smoothing error, which ~~is estimated to be 30~~

Formatted: Normal
Formatted: Font: Times New Roman
Formatted: Font: Times New Roman
Formatted: Font: Times New Roman
Formatted: Font: Times New Roman
Formatted: Font: Times New Roman
Formatted: Font: Times New Roman
Formatted: Font: Times New Roman
Formatted: Font: Times New Roman
Formatted: Font: Times New Roman
Formatted: Font: Times New Roman
Formatted: Font: Times New Roman
Formatted: Font: Times New Roman
Formatted: Font: Times New Roman
Formatted: Font: Times New Roman
Formatted: Font: Times New Roman
Formatted: Font: Times New Roman
Formatted: Font: Times New Roman
Formatted: Font: Times New Roman
Formatted: Font: Times New Roman
Formatted: Font: Times New Roman
Formatted: Font color: Black
Formatted: Normal, Border: Top: (No border), Bottom: (No border), Left: (No border), Right: (No border), Between : (No border), Tab stops: 3.13", Centered + 6.27", Right

ppb. In Equation 5a, we first apply the AIRS Averaging kernel tocovariance of the aircraft measurement to account for$h_c A_{cc}\left(x_c - x_a^c\right)$ (Rodgers, 2000), where the AIRS sensitivity:covariance of $\left(x_c - x_a^c\right)$ is the a priori covariance, S_a^{xx}. The smoothing error is:

$$\hat{x}_{aircraft}^{c} = \mathbf{h_c x_a} + \mathbf{h_c A_{cc}}\left(\mathbf{x_{aircraft}^{c} - x_a^c}\right) + \mathbf{h_c A_{cs}}\left(\mathbf{x_{aircraft}^{s} - x_a^s}\right) \quad \textbf{(5a)}$$

Smoothing error = $h_c A_{cc} S_a^{xx} A_{cc}^T h_c^T$ **(5)**

We estimate the smoothing error for the partial column XCH_4 VMR within the pressure levels measured by the aircraft to be 30 ppb, using Eq. 5. This estimate strongly depends on S_a^{xx}, the a priori covariance, which is the same as in Worden et al. (2012); briefly 5% diagonal variability with correlations in pressure set from the MOZART model. In Equation 6a, we apply the AIRS Averaging kernel to the aircraft measurement to fully account for the AIRS sensitivity:

$$\hat{x}_{aircraft}^{c} = h_c x_a + h_c A_{cc}\left(x_{aircraft}^{c} - x_a^c\right) + h_c A_{cs}\left(x_{aircraft}^{s} - x_a^s\right) \quad \textbf{(6a)}$$

$$\hat{x}_{aircraft}^{c} = h_c x_a + h_c A_{cc}\left(x_{aircraft}^{c} - x_a^c\right) \quad \textbf{(6b)}$$

One issue is that we do not actually have aircraft observations in the "s" part of the atmosphere, $\mathbf{x_{aircraft}^{s}}$ $x_{aircraft}^{s}$, which is used in the second term of Eq. 5a6a. We have aircraft observations in the "c" part of the atmosphere only, so we apply the Averaging Kernel to this part of the atmosphere only:

$$\hat{x}_{aircraft}^{c} = \mathbf{h_c x_a} + \mathbf{h_c A_{cc}}\left(\mathbf{x_{aircraft}^{c} - x_a^c}\right) \quad \textbf{(5b)}$$

. Equation 5a6a accounts for all of the AIRS smoothing error, whereas Equation 5b6b (the equation used in this work, other than Section 3.3) only accounts for the smoothing error from the part of the atmosphere measured by the aircraft profile. The difference from Eqs. 5a6a and 5b6b is discussed in Section 3.3.

The expected difference Equation 7a is the predicted bias between $\hat{x}_c$ (the measured AIRS value) and $\hat{x}_{aircraft}^{c}$ (the aircraft value with the AIRS Averaging kernel applied)), and is calculated fromthe expected difference of Eqs. 4 and 5b:

$$\mathbf{E}\left\|\left(\hat{x}_c - \hat{x}_{aircraft}^{c}\right)\right\| = \mathbf{h_c}\left(\mathbf{A_{cb}}\mathbf{S_a^{bb}}\mathbf{A_{cb}^T} + \mathbf{A_{cy}}\mathbf{S_a^{yy}}\mathbf{A_{cy}^T} + \mathbf{A_{cs}}\mathbf{S_a^{ss}}\mathbf{A_{cs}^T} + \mathbf{S_m^{cc}}\right)\mathbf{h_c^T} \quad \textbf{(6)}$$

Formatted: Normal
Formatted: Font: Times New Roman
Formatted: Font: Times New Roman
Formatted: Font: Times New Roman
Formatted: Font: Times New Roman
Formatted: Font: Times New Roman
Formatted: Font: Times New Roman
Formatted: Font: Times New Roman
Formatted: Font: Times New Roman
Formatted: Font: Times New Roman
Formatted: Font: Times New Roman
Formatted: Font: Times New Roman
Formatted: Font: Times New Roman
Formatted: Font: Times New Roman
Formatted: Font: Times New Roman
Formatted: Font: Times New Roman
Formatted: Font: Times New Roman
Formatted: Font: Times New Roman
Formatted: Font: Times New Roman
Formatted: Font color: Black
Formatted: Normal, Border: Top: (No border), Bottom: (No border), Left: (No border), Right: (No border), Between : (No border), Tab stops: 3.13", Centered + 6.27", Right

~~The matrix $\mathbf{S_a}$ term describes the *a priori* uncertainty of methane, interferents, or systematic parameters, which propagate into the~~6b. Equation 7b is the covariance of Eq. 7a, and estimates the predicted error ~~in the first 3 terms:~~:

$$E(\hat{x}_c - \hat{x}^c_{aircraft}) = h_c G_c K^b E(b_{error}) + h_c A_{cy} E(\hat{y} - y_a) + h_c A_{cs} E(\hat{x}_s - x_s) + h_c G_c E(n_{error}) \quad \textbf{(7a)}$$

$$E||\ (\hat{x}_c - \hat{x}^c_{aircraft})|| = h_c(G_c K^b S_a^{bb} K_b^T G_c^T + A_{cy} S_a^{yy} A_{cy}^T + A_{cs} S_a^{ss} A_{cs}^T + S_m^{cc}) h_c^T \quad \textbf{(7b)}$$

Eq. 7a represents the propagation of mean biases from: (1) ~~$\mathbf{A_{cb}S_a^{bb}A_{cb}^T}$ describes systematic error~~non-retrieved parameters and assumptions, e.g. ~~due to~~ spectroscopy ~~and calibration; these likely impart biases into the AIRS measurement which are characterized during validation, (b),~~ (2) ~~$\mathbf{A_{cy}S_a^{yy}A_{cy}^T}$ describes the "cross-state error", the effect of~~ jointly retrieved parameters ~~like,~~ e.g. temperature ~~onto methane, (3) $\mathbf{A_{cs}S_a^{ss}A_{cs}^T}$ describes, (y), (3) "stratospheric", describing~~ the impact of the part of the atmosphere not covered by the aircraft on the measured ~~section: this must be included because the AIRS measurement sees a combination of both parts of the atmosphere and cannot completely disentangle them. The final term, $\mathbf{S_m^{cc}}$, is the measurement error, which is the propagation of radiance error into the retrieved parameters, and is $\mathbf{G_c}$ $\mathbf{S_n}$ $\mathbf{G_c^T}$, where $\mathbf{G_c}$ is the gain matrix and $\mathbf{S_n}$~~part (x_s), or (4) measurement errors (n) into biases of $\hat{x}_c$. The mean bias from 7a is difficult to characterize theoretically and is characterized during validation, and assumed to be primarily from the first term (e.g. spectroscopy). Equation 7b is the covariance of the ~~radiance error, in our case, a diagonal matrix.~~ terms in 7a, where e.g. the covariance of b_{error} is S_a^{bb}. Equations 7b represent the "observation covariance". The square root of 7b is the predicted observation error. Although Eq. 7b has overall zero bias, it can produce regional and temporal biases, e.g. as seen in Connor et al. (2016), where these biases approach zero over long enough spatial or temporal scales. The error covariances all represent fractional errors, in log(VMR). ~~The~~Because the retrieved quantity log(VMR), the error in ppb is approximately the fractional error times the methane value in ppb.

For the purpose of evaluating the AIRS methane measurement uncertainties and comparing the AIRS methane to aircraft in situ measurements we refer to the four terms on the right side of Eq. ~~6~~7b as:

1) ~~$\mathbf{S_b^{cc}}$~~ S_b^{cc} is the systematic error due to terms that are not accounted for in the retrieval state vector, such as spectroscopy and calibration; these terms are estimated by comparisons with the aircraft data. A pressure-dependent bias correction, described in Section 3.4, of approximately -60 ppb is used to correct this systematic bias.
2) ~~$\mathbf{A_{cy}S_a^{yy}A_{cy}^T}$~~ $A_{cy} S_a^{yy} A_{cy}^T$, the "cross-state", which is included in the MUSES-AIRS methane estimate product files, and is the propagation of temperature, water vapor, and cloud errors into AIRS. The errors in the retrieved temperature and water vapor at nearby location are correlated over short spatio-temporal scales, as described in Section 4, and so this error does not reduce with averaging nearby observations. However, monthly or seasonal

Formatted: Normal

Formatted: Font: Times New Roman

Formatted: Font: Times New Roman

Formatted: Font: Times New Roman

Formatted: Font: Times New Roman

Formatted: Font: Times New Roman

Formatted: Font: Times New Roman

Formatted: Font: Times New Roman

Formatted: Font: Times New Roman

Formatted: Font: Times New Roman

Formatted: Font: Times New Roman

Formatted: Font: Times New Roman

Formatted: Normal, Outline numbered + Level: 1 + Numbering Style: 1, 2, 3, … + Start at: 1 + Alignment: Left + Aligned at: 0.25" + Indent at: 0.5", Border: Top: (No border), Bottom: (No border), Left: (No border), Right: (No border), Between : (No border)

Formatted: Font: Times New Roman, Font color: Black

Formatted: Font: Times New Roman, Font color: Black

Formatted: Font color: Black

Formatted: Normal, Border: Top: (No border), Bottom: (No border), Left: (No border), Right: (No border), Between : (No border), Tab stops: 3.13", Centered + 6.27", Right

averages reduces cross-state error, because systematic errors from temperature / water / cloud can be assumed to vary pseudo-randomly over larger time scales. ~~We estimate this error as ~ 21 ppb (see next paragraph).~~

3) ~~$\mathbf{A_{cn}S_a^{nn}A_{cn}^T}$~~ $A_{cs}S_a^{ss}A_{cs}^T$ is the "validation uncertainty" due to knowledge uncertainty of the stratosphere although this may also contain other levels that are also not measured by the aircraft. This is the smoothing error which cannot be removed from the comparisons because the aircraft does not make measurements at the "~~n~~" (~~not measured~~)s" ("stratospheric") levels. We estimate this validation ~~error~~uncertainty as ~~16~~10 ppb (~~see next section~~). estimated in Section 3.3). This estimate depends on the accuracy of the model used to extend the aircraft profile during the validation process and was estimated for the model that we used in validation.

4) ~~$\mathbf{S_m^{cc}}$~~ S_m^{cc} the "measurement" error, which is included in the AIRS methane estimate product files. The measurement error is random and is expected to reduce as the inverse square root of the number of observations averaged. We estimate this error as ~18 ppb (~~see next paragraph~~)using the last term of Eq. 7b and shown in Fig. 3) and find it to be a random error that reduces with averaging.

Figure 3 shows the predicted errors for the AIRS partial column ~~matching~~XCH_4 VMR within the pressure levels measured by the aircraft ~~measurements.~~ The measurement error (light green) is 18 ppb~~, the cross-state error is 21 ppb (red minus green in quadrature),~~ (from the last term of Eq. 7b) and the total error for a single observation (including smoothing error) is 41 ppb. ~~The errors not shown in this plot are~~A component of the ~~validation~~total error, the cross-state error, is estimated ~~in the next section, and systematic error, which we remove with a bias correction in Section 3.4.~~ as 21 ppb (from Eq. 7b).

3.3 Estimating validation ~~error~~uncertainty due to aircraft not measuring the stratosphere

A typical aircraft profile will only measure part of the troposphere and rarely measure into the stratosphere. However, the AIRS methane profile measurements are sensitive to methane variations over the whole atmosphere as shown by the averaging kernel matrix in Figure 2. Similarly, the true state in the troposphere influences retrieved values in the stratosphere. Options for dealing with this are a) extending the true with the AIRS prior or b) extending the true with a model profile value. ~~Note that models in general have a positive bias in the extratropical stratosphere (Patra et al., 2011). In GEOS-Chem 4x5, the column bias is shown in Figure 2c of Turner et al. (2015) and further discussed in Maasakkers (2019), which finds a bias in the stratosphere.~~

This section estimates this uncertainty by calculating the difference of ~~$\boldsymbol{x}^{\boldsymbol{c}}_{\boldsymbol{aircraft}}$~~ $x^c_{aircraft}$ for Eq. ~~5a~~6a minus Eq. ~~5b~~6b when extending the aircraft using two different "true" profiles taken from two different global atmospheric chemistry models, the Laboratoire de Météorologie Dynamique (LMDz) model (e.g. Folberth et al., 2006) model and the Goddard Earth Observing System (GEOS-Chem) model (e.g. Maasakkers et al., 2019). So, if the model value equaled the AIRS prior in the

Formatted: Normal

Formatted: Font: Times New Roman, Font color: Black

Formatted: Font: Times New Roman, Font color: Black

Formatted: Font: Times New Roman, Font color: Black

Formatted: Font: Times New Roman

Formatted: Font: Times New Roman, Font color: Black

Formatted: Font: Times New Roman, Font color: Black

Formatted: Font: Times New Roman, Font color: Black

Formatted: Font: Times New Roman, Font color: Black

Formatted: Font: Times New Roman

Formatted: Font: Times New Roman

Formatted: Font: Times New Roman

Formatted: Font: Times New Roman

Formatted: Font: Times New Roman

Formatted: Font: Times New Roman

Formatted: Font: Times New Roman

Formatted: Font: Times New Roman

Formatted: Font color: Black

Formatted: Normal, Border: Top: (No border), Bottom: (No border), Left: (No border), Right: (No border), Between : (No border), Tab stops: 3.13", Centered + 6.27", Right

stratosphere, this difference would be zero. The differences for $x^{c}_{aircraft}$ $\chi^{c}_{aircraft}$ from LMDz model and GEOS-Chem are shown in Figure 4 for all HIPPO ocean and land data; these differences show that model/model differences in the stratosphere can contribute significantly to the differences between AIRS and aircraft validation.

These differences provide an estimate for how knowledge error in the stratosphere projects to uncertainties in our methane retrievals. For example, this uncertainty varies with latitude, similar to the residual bias between the AIRS estimate and aircraft (next section). Furthermore, the variability over small latitudinal ranges of 10 degrees or less suggests that the random part of the stratospheric error is smaller than this latitudinal variability. Our 16 ppb estimate for this error is similarthe average of these two errors, 10 ppb, and places an upper bound on the ability to validate AIRS CH_4. Our estimate for this error agrees with the 10 ppb estimate for the impact of stratospheric uncertainty on column estimates from aircraft profiles (Wunch et al., 2010). Appendix A shows further analysis of mean differences of AIRS minus aircraft for different profile extension choices. The bias varies by ~ 5 ppb for different profile extension choices when comparing at 700 hPa, ~10 ppb for different profile extension choices when comparing at 500 hPa, and ~11 ppb for different profile extension choices when comparing the column above 750 hPa.

The methane profile has a strong variable negative vertical gradient in the stratosphere. Models in general have a positive bias in the extratropical stratosphere (Patra et al., 2011). In GEOS-Chem 4x5, the column bias is shown in Figure 2c of Turner et al. (2015) and further discussed in Maasakkers (2019), which resolves the bias to the stratosphere, and model stratospheric accuracy is an active research area (Ostler et al., 2016; Maasakkers et al., 2019).

3.4 Bias Correction

AIRS CH_4 shows a persistent high bias of 25 to 90 ppb versus aircraft observations in Fig. 65. Previous studies using remotely sensed measurements suggest that a bias correction to the AIRS methane profile measurement must account for the vertical sensitivity (e.g. Worden et al., 2011). For example, in the limit where the AIRS measurement is perfectly sensitive to the vertical distribution of methane, the bias correction could be a simple scaling factor. However, in the limit where the AIRS measurement is completely insensitive (e.g. DOFS = 0.0) then the bias correction is zero. We therefore use the bias correction approach described in Worden et al. (2011), which passeswhere a bias correctionprofile (which varies by pressure) is passed through the averaging kernel to account for the AIRS sensitivity. , as seen in Eq. 8. The form of the bias profile, δ_{bias} is set in Eq. 9.

We use HIPPO-4 observations to set a bias correction which we then evaluate with the other HIPPO campaigns and NOAA aircraft network data. HIPPO-4 was selected as it covers a wide range of latitudes and so that the bias correction can be set and tested with two independent datasets. To set the bias, we use Eq. 56b to estimate the aircraft observation as seen by AIRS,

Formatted: Normal

Formatted: Font color: Black

Formatted: Normal, Border: Top: (No border), Bottom: (No border), Left: (No border), Right: (No border), Between : (No border), Tab stops: 3.13", Centered + 6.27", Right

then compare this to AIRS observations. The result (by pressure level) is shown in Table 1. Then a bias was applied to AIRS using Eq. ~~7~~8, with the bias term δ_{bias} in the form of Eq. ~~8~~9.

~~$ln(\hat{x}_{corrected}) = ln(\hat{x}_{orig}) + A(\delta_{bias})$ (7)~~

$$\hat{x}_{corrected} = \hat{x}_{orig} + A\delta_{bias} \quad \textbf{(8)}$$

Where ~~ln() is the natural log,~~$\hat{x}$ = ln(VMR), because the retrieved quantity is ln(VMR), δ_{bias} is a vector, and A is the averaging kernel matrix for $\hat{x}$ = ln(VMR). We fit a single bias function for all AIRS measurements by minimizing the difference between the AIRS and HIPPO-4 with ~~δ_bias~~δ_{bias} constrained to have a slope with pressure, and two pressure domains. We specify that ~~δ_bias~~δ_{bias} cannot jump more than 0.05 (5%) between the two domains.

$$\delta_{bias} = c + dP \text{ (P > P}_o\text{)}$$
$$\delta_{bias} = e + fP \text{ (P < P}_o\text{)} \quad \textbf{(~~8~~9)}$$

where P is pressure in hPa. The optimized bias correction parameters were: c = 0.0; d = - 6.1e-5; ~~Po~~P_0=400 hPa; e=-0.09; f=0.00018. This bias correction results are shown for HIPPO-4; HIPPO-1,2,3,5; and NOAA observations in Table 1. The remainder of the paper, unless specified, uses data bias-corrected by Eqs. ~~7~~8 and ~~8~~9.

Figure ~~5~~6 shows the effect of bias correction on the average of all HIPPO 1,2,3,5 AIRS profiles. The bias correction improves the mean AIRS / aircraft difference and improves the pressure-dependent skew in the bias (Table 1). The HIPPO data is shown before and after the AIRS averaging kernel is applied (using Eq. ~~5~~6b), which has the effect of bringing the HIPPO observations towards the AIRS prior. This is to match the imperfect sensitivity of satellite-based observations, which are similarly influenced by the prior.

4 Evaluation against aircraft data ~~by~~versus latitude

4.1 Comparison of aircraft observations with and without bias correction

Figure ~~6~~5 shows a comparison between all AIRS measurements within 50 km and 9h of an aircraft measurement ~~for~~ and the aircraft measurement. The quantity compared is the partial column XCH_4 VMR within the pressure levels measured ~~by~~from the aircraft. There is a mean bias of 57 ppb overall, ~~56~~52 ppb for ocean and ~~64~~76 ppb for the land. The RMS difference is ~~27~~26 ppb. Furthermore, there appears to be latitudinal variations in the bias. For example, the mean difference between the

Formatted: Normal

Formatted: Font: 10 pt

Formatted: Font color: Black

Formatted: Normal, Border: Top: (No border), Bottom: (No border), Left: (No border), Right: (No border), Between : (No border), Tab stops: 3.13", Centered + 6.27", Right

AIRS and aircraft over the ocean for latitudes less than 20 S is ~74 ppb and for latitudes between 20 S and 20 N this bias is ~ 56 ppb.

Figure 7 shows the same comparisons as Fig. ~~6~~5 after bias correction (described in Section 3.4). The mean bias is 1 ppb, and the RMS difference is 24 ppb. The overall land bias is ~~13 ppb, and the overall ocean bias is 1 ppb (shown in Table A.1).~~12 ppb, and the overall ocean bias is -2 ppb. The bias calculated in Fig. 7 is weighs every point equally. Table A.1 shows a slightly different result for these biases, where the bias is calculated by campaign, then averaged over all campaigns. In Table A.1 the partial column XCH_4 VMR within the pressure levels measured by the aircraft has a bias of 16 ppb for land, and -2 ppb for ocean. Note that the HIPPO land observations are primarily in Australia, New Zealand, and North America, whereas the ocean comparisons are in the mid-Pacific, as seen in Fig. 1. We expect the RMS difference to be similar to the observation error, as the terms that make up the observation error are the primary source of variability in the observations (e.g. Worden et al., 2017b). The predicted observation error from Fig. 3, is 27 ppb, and is consistent with the RMS difference seen here, ~~24~~23 ppb. However, knowledge of the stratosphere / validation ~~error~~uncertainty is potentially a large component of the latitudinal variability in the difference seen in the bottom panel of Fig. 7.

We also compare to NOAA aircraft network and ATom observations and find similar results as HIPPO. Figure 8, discussed in Section 4.2, shows ATom results, and Figure 9, discussed in Section 4.2, shows comparisons to a NOAA aircraft time series. The biases for different pressure ranges, campaigns, and surfaces is shown in Table A.1. Table A.3 shows the standard deviation of AIRS minus validation by pressure and surface type, for single observations, daily, and seasonal averages.

4.2 Errors in averaged AIRS data

Satellite data are typically averaged in order to improve the precision of a comparison between data and model. However, as shown in the previous figure, these data contain errors that vary with latitude. For example, knowledge error of the true profile in the stratosphere as well as errors in the jointly retrieved AIRS temperature and water vapor retrievals have both a random and a bias component, both of which vary with latitude. The bias component is approximately the same for all AIRS methane measurements taken ~~at roughly~~on the same ~~location and time~~day within 50 km, as we do not expect large variations in temperature and water vapor errors over these scales, which we presume to be a driver of these correlated errors. To quantify the component of the accuracy that cannot be reduced by averaging, we compare averages of AIRS measurements to HIPPO and ATom measurements. We average ~~the daily matches, which contain at least 9~~over 1 day, the AIRS observations matching a single HIPPO or ATom measurement, within +-50 km and 9 hours of the measurement. ~~The number of AIRS observations averaged ranges from 9 to 53 and averages 20.~~ We specify that there needs to be at least 9 AIRS observations for each comparison so that the systematic error, and not the precision (or measurement error~~),~~), is the dominant term. These daily AIRS averages contain, on average, 20 AIRS observations. Figure 8 shows the ~~average~~ predicted error, assuming that the

Formatted: Normal

Formatted: Font color: Black

Formatted: Normal, Border: Top: (No border), Bottom: (No border), Left: (No border), Right: (No border), Between : (No border), Tab stops: 3.13", Centered + 6.27", Right

error is random, ~~e.g. if 20 observations were~~which is calculated by dividing the single observation error (24 ppb RMS shown in Fig. 7) by the square root of the number of observations that are averaged~~, this would equal 24 / √20 ppb or ~ 5~~. The mean predicted error for the averaged data, assuming random errors, is 6 ppb. The actual standard deviation between the averaged AIRS and HIPPO or ATom data is ~17 ppb, which is much larger and indicates that the errors within 1 day and 50 km are correlated. Note that same-colored adjacent points (i.e. adjacent observations from the same campaign) often show similar biases. Because this RMS difference is much larger than what is expected if the errors were purely random, this shows the presence of systematic errors, either in the AIRS data or in the validation ~~error~~uncertainty. We therefore report 17 ppb as the limiting error when averaging AIRS data within one-degree grids and 1 day for the purpose of comparing to models or other methane profiles.

On the other hand, averaging AIRS data seasonally can reduce the error further because geophysical errors from as temperature and water vapor vary over longer time scales. We demonstrate this aspect of the AIRS uncertainties by comparing averaged AIRS data to the NOAA aircraft methane profiles taken off the coast near Corpus Christi, Texas (27.7N, 96.9W, site TGC). We screen for at least 3 observations per day, less than the 9 observations/day used for HIPPO / ATom daily averages in order to get enough daily averages to explore how the errors reduce with monthly and seasonal averages, since the aircraft make 1-2 measurements per month. Figure 9 shows daily, monthly, 90-day, and seasonal averages of the partial column ~~matching~~XCH_4 VMR within the pressure levels measured from the aircraft ~~measured column~~ at TGC. The seasonal averages are created by converting all AIRS/aircraft matched pairs to 2012 by adding 5.4 ppb per year multiplied by (year minus 2012~~), then averaging all values within each month. Similarly)~~ to ~~the findings~~account for ~~HIPPO and ATom,~~ the mean annual growth rate. The growth rate of 5.4 ppb/year is the mean increase during the AIRS record time period (2002-2019) estimated from the NOAA Global Monitoring Laboratory global surface measurements (https://esrl.noaa.gov/gmd/ccgg/trends_ch4/). Since we are converting matched pairs of aircraft and AIRS to 2012, the differences between these matched pairs is unaffected by the accuracy of the conversion to 2012.

4.2.1 Daily average errors at TGC

We look at daily ~~error is~~ averages versus aircraft data and find a similar result as that found with comparisons to ATom and HIPPO: daily averages have much larger errors than would be predicted ~~from the observation error with the assumption of randomness.~~if random errors are assumed. The standard deviation of (AIRS minus aircraft) at TGC is 24 ppb ~~(~~, the standard deviation for ~~single~~(daily AIRS ~~observation, not shown),~~average minus aircraft) is 11.5 ppb ~~(for daily AIRS average, (Figure~~, as seen in Fig. 9a~~)). The~~, and the predicted error ~~with the assumption that~~for daily averages, assuming randomness in the error ~~is random~~, is 6.0 ppb. Therefore, similarly to ~~the~~ ATom and HIPPO ~~findings, the,~~ errors within ~~small geophysical region are~~ 1 day and 50 km contain 11.5 ppb correlated ~~and do not~~error.

4.2.2 Monthly average ~~as~~errors at TGC

Formatted: Normal

Formatted: Font: Bold

Formatted: Font color: Black

Formatted: Normal, Border: Top: (No border), Bottom: (No border), Left: (No border), Right: (No border), Between : (No border), Tab stops: 3.13", Centered + 6.27", Right

The NOAA aircraft measurements are usually taken about twice per month. The standard deviation of (monthly AIRS average minus aircraft) is 8.2 ppb (Figure 9b) for months containing more than 1 aircraft observation. This is compared to the daily error divided by the square root of the number of days averaged, 8.0 ppb. Therefore, errors for observations. However, next, we try averaging multiple days within 1 ~2 weeks apart are uncorrelated.

4.2.3 3-month, and find a standard deviation of for monthly average errors at TGC

We average over 3-month scales, where averages ofmust have at least 23 days of 8.2 ppb (Figure 9b), and the . The standard deviation of (3-month averages containing at least 3 days,AIRS average minus aircraft) is 6.2 ppb (Figure 9c). These agree with the. The predicted errors of 8.0 and 6.0 ppb, respectively, by error, taking the daily standard deviation (11.5 ppb) daily error and dividing by the square root of the number of days averaged. The seasonal, is 6.0 ppb. Therefore, errors for 3-month averages are ~uncorrelated.

4.2.3 Seasonal cycle average, which is a monthly errors at TGC

We average of all matched pairs within each month from any year, has. (AIRS minus aircraft) for these averages, have a standard deviation of 5.9 ppb, whereas the predicted error, from the daily average divided by the square root of number of observations, is 4.2 ppb.

Appendix A, **4.2.4 Summary of average errors at TGC**

To summarize, averaging AIRS observations within one day reduces the error versus aircraft, but correlated errors prevent daily averaged errors from dropping below 11.5 ppb. Averaging daily averages over 1 or 3 months equals the daily error divided by the square root of the number of days averaged, indicating that errors are random in this domain. However, averaging months from multiple years, does not reduce the error below 6 ppb, either due to correlated errors, or validation uncertainty.

4.2.5 Summary of errors at all NOAA aircraft sites

Table A.3 in Appendix A shows the single-observation standard deviation for all NOAA ESRL stations, for ocean and land AIRS observationsaircraft sites. The ocean vs. land observations show similar values, with land and ocean standard deviations within 2 ppb. A single land observation has a standard deviation versus aircraft observations of 23 ppb for the partial column XCH_4 VMR within the pressure levels measured from the aircraft, in agreement with predicted observation error of 23 ppb. The standard deviation for daily observationsaverages is 15.2 ppb, whereas. This can be compared to the predicted error, using 23 ppb divided by the square root for the daily averages, assuming randomness, of the number of observations averaged, is 5.9 ppb, indicated. This indicates that there are correlated (non-random) errors on the order of 15 ppb when averaging nearby observations within 50 km and 1 day. The monthly standard deviation is 10.9, in reasonable agreement with the predicted of 9.4 ppb, (from the daily average standard deviation divided by the number of observations averaged.). The seasonal cycle

Formatted: Normal

Formatted: Font: Bold

Formatted: Font: Bold

Formatted: Pattern: Clear (Custom Color(RGB(255,242,204)))

Formatted: Pattern: Clear (Background 1)

Formatted: Font color: Black

Formatted: Normal, Border: Top: (No border), Bottom: (No border), Left: (No border), Right: (No border), Between : (No border), Tab stops: 3.13", Centered + 6.27", Right

average, which is a monthly average of all matched pairs from all years, has a standard deviation of 7.7 ppb, which is similar to the predicted error of 6.9 ppb~~,~~ (from the daily average divided by the square root of number of observations~~.~~). We find that estimating the error as the daily standard deviation divided by the square root of the number of days averaged is a reasonable estimate of the actual error.

4.2.6 The bias and bias uncertainty

The bias is estimated by calculating the mean bias for each campaign or station separately, then calculating the mean and standard deviation for all campaigns / stations. The bias versus HIPPO is 0 ± 4 ppb. The bias versus ATom is 3 ± 4 ppb. The bias versus NOAA measurements is 9 ± 7 ppb.

5 Discussion and Conclusions

We validate single-footprint AIRS methane by comparing 27,000 AIRS methane retrievals to 396 aircraft profiles from the HIPPO campaign, 719 profiles from the NOAA ~~ESRL~~GML aircraft network, and 289 aircraft profiles from the ATom campaign, taken across a range of latitudes, longitudes, and times. The AIRS methane retrievals are derived using the MUSES optimal estimation algorithm that has previously been applied to Aura TES radiances (e.g. Fu et al., 2013). After adjusting the aircraft profile to account for the AIRS sensitivity (using the averaging kernel and a priori ~~-~~profile), we compare the mean methane value over the aircraft profile to the mean methane from the AIRS profile over the same altitude (or pressure) range. We use a subset of validation data to derive a pressure-dependent bias correction on the order of -60 ppb, and test this on an independent set of validation data. After the bias correction, we report a bias of 0 +/- 10 ppb. The bias between AIRS and aircraft varies with pressure and location, as seen in Appendix A.

After applying the bias correction, from Eq. ~~7~~8 and ~~8~~9, the RMS difference between the AIRS and aircraft data of the partial column ~~matching~~XCH_4 VMR within the pressure levels measured by the aircraft of ~22 ppb is consistent with the mean observation error, composed of random error from noise and the cross-state errors from jointly retrieved temperature, water vapor, clouds, and surface parameters that are projected onto the AIRS methane retrieval. The extent to which the aircraft profiles used here can be utilized as "truth" for the purposes of validation is limited by knowledge of the methane profile above the aircraft profile (referred to here as "validation ~~error~~",uncertainty"), which limits our knowledge of "truth" to within about ~~16~~10 ppb. This uncertainty is consistent with the location-dependent bias in the satellite/aircraft comparisons which can vary by ~10 ppb.

We quantify the AIRS minus validation standard deviation for single observations, daily averages (within 50 km of the validation location), monthly averages, and seasonal averages for data bias corrected using Eqs. 7 and 8. The AIRS minus validation standard deviations are: 24 ppb (single AIRS footprint), 17 ppb (daily AIRS averages within 1 degree latitude and

Formatted: Normal

Formatted: Font color: Black

Formatted: Normal, Border: Top: (No border), Bottom: (No border), Left: (No border), Right: (No border), Between : (No border), Tab stops: 3.13", Centered + 6.27", Right

longitude), 10 ppb ("monthly" AIRS averages), 9 ppb (3-month AIRS average), and 7 ppb (seasonal cycle average). The errors on averaged AIRS data are likely an upper bound on the AIRS error, due to the uncertainty in the validation. The single-footprint and daily average standard deviations for different pressure ranges and surface types are shown in Appendix A. We recommend using the standard deviations in this paragraph as the error budget for the specified averaged quantities.

These results can be compared to AIRS v6 validation by Xiong et al. (2015), which validated AIRS CH_4 retrieved from cloud-cleared radiances on the 9-footprint 45 km field of regard. Xiong et al. (2015) finds AIRS standard deviations versus HIPPO of 0.9% (16 ppb) for pressures between 575 and 777 hPa, 1.2 % (18 ppb) standard deviation for pressures between 441 and 575 hPa, and 1.6% (29 ppb) between 343 and 441 hPa. Xiong et al. (2015) also found a pressure-dependent bias, with a -25 ppb bias near the top of the troposphere, and a high 5 ppb bias near the mid-Troposphere.

5 Appendix A: Biases and standard deviations for different stations, campaigns, pressures, and surface types

We characterize the bias versus validation data by station, campaign, and pressure level. Table A.1 shows biases versus validation data, after bias correction with ~~Eq. 7~~Eqs. 8 and 9. In the HIPPO comparisons, the biases are generally smaller than about 10 ppb. There is no overall pattern in the bias by season. The land data is biased higher than ocean for HIPPO comparisons (about +20 ppb). However, note that the land observations versus HIPPO are primarily in Australia and New Zealand, whereas the ocean comparisons are in the mid-Pacific.

The NOAA aircraft network comparisons are sorted by site. Many NOAA aircraft locations are at land/ocean interfaces, allowing a more direct comparison of the land/ocean biases. On average, the AIRS land observations are 0-5 ppb higher than AIRS ocean observations at the different pressures and pressure ranges. The overall bias of AIRS versus NOAA aircraft is +7.1 ppb, whereas AIRS versus HIPPO is 4.4 ppb for the partial column ~~matching~~XCH_4 VMR within the pressure levels measured by the aircraft ~~observations.~~. This is consistent with AIRS land having a high bias versus ocean of 0-5 ppb.

The standard deviation of the bias for the different campaigns is a useful quantity as it is an indication of systematic error. The standard deviation of the bias varies from 4 ppb to 9 ppb for the different ~~pressures and campaigns.~~ vertical quantities.

Table A.2 shows the mean bias for AIRS minus NOAA ~~ESRL~~GML aircraft for land and ocean AIRS observations.~~s~~ The different rows extend the aircraft using the AIRS prior, the CarbonTracker model (from https://www.esrl.noaa.gov/gmd/ccgg/carbontracker-ch4/ or the GEOS-Chem model (both are extended through 2018 using 2.5% secular increase). The goal of this table is to approximate the influence of the profile extension on the validation accuracy.

Table A.3 shows the standard deviation for AIRS observations minus validation data for land / ocean for different pressure ranges for both single observations and AIRS averages. The mean bias at each site is subtracted prior to calculating the

Formatted: Normal

Formatted: Font color: Black

Formatted: Normal, Border: Top: (No border), Bottom: (No border), Left: (No border), Right: (No border), Between : (No border), Tab stops: 3.13", Centered + 6.27", Right

standard deviation. This table shows the standard deviations for single observations and averaged quantities. The predicted error for the daily average is the observation error divided by the square root of the number of observations, and is much smaller than the actual standard deviation, indicating correlated errors. The predicted error for the monthly, 3-month, and seasonal cycle averages is the daily standard deviation divided by the square root of the number of days averaged and ~agrees with the actual standard deviation for the partial column. XCH_4 VMR within the pressure levels measured by the aircraft. The location-dependent biases are subtracted from AIRS prior to calculating the standard deviation in all but the last two rows. The last two rows shows the standard deviations without subtracting the location-dependent biases, which increases the partial column standard deviation from about 8 ppb to about 9 ppb.

Author contributions: SSK and JRW are responsible for the study design, data analysis, and manuscript writing; VHP was responsible for data analysis and manuscript editing; DF was responsible for implementing AIRS into the MUSES retrieval system; SCW and BCD were responsible for HIPPO Picarro CH_4 data; KM and CS were responsible for the ATom Picarro CH_4 data; EJD, CS, and KM were responsible for NOAA ESRLGML aircraft data; AL, IP, YH, and KC were responsible for implementation of the fast RT, OSS, used in this work. YY provided LMDZ model runs. DJ provided guidance on GEOS-Chem model runs.

Acknowledgements: This work is supported by NASA ROSES Aura Science Team NNN13D455T. Part of this research was carried out at the Jet Propulsion Laboratory, California Institute of Technology, under a contract with the National Aeronautics and Space Administration. The NOAA ESRLGML aircraft observations were obtained from http://dx.doi.org/10.25925/20190108 and supported by NOAA. The HIPPO aircraft data were obtained from http://www.eol.ucar.edu/projects/hippo/ and supported by NOAA and NSF. Thanks to Bruce Daube, Eric Kort, Jasna Pittman, Greg Santoni and others for QCLS CH_4 data collection/processing. The ATom aircraft data were obtained from https://daac.ornl.gov/ATOM/ and supported by NASA. The GEOS-Chem model output is described in Worden et al. (2013a). Thank you to helpful comments and feedback from J.D. Maasakkers.

Data Availability: AIRS methane data are available at: https://avdc.gsfc.nasa.gov/pub/data/satellite/Aura/TES/.AIRS/TROPESS/YEAR/.... Note that the field "original_species" should be used with the bias correction described in this paper. The specific datasets used in this work are archived at: https://drive.google.com/file/d/1crNs-QcOzbjiZUiTyRiTEsFORFTbODAW/view?usp=sharing.

Formatted: Normal

Formatted: Font color: Black

Formatted: Normal, Border: Top: (No border), Bottom: (No border), Left: (No border), Right: (No border), Between : (No border), Tab stops: 3.13", Centered + 6.27", Right

References

Alvarado, M. J., Payne, V. H., Cady-Pereira, K. E., Hegarty, J. D., Kulawik, S. S., Wecht, K. J., Worden, J. R., Pittman, J. V. and Wofsy, S. C.: Impacts of updated spectroscopy on thermal infrared retrievals of methane evaluated with HIPPO data, Atmospheric Measurement Techniques, 8(2), 965–985, doi:10.5194/amt-8-965-2015, 2015.

Brasseur, G. P., Hauglustaine, D. A., Walters, S., Rasch, P. J., Muller, J. F., Granier, C., and Tie, X. X.: MOZART, a global chemical transport model for ozone and related chemical trac- ers 1. Model description, J. Geophys. Res.-Atmos., 103, 28265–28289, 1998.

Bowman, K. W., Rodgers, C. D., Kulawik, S. S., Worden, J., Sarkissian, E., Osterman, G., Steck, T., Lou, M., Eldering, A. and Shephard, M.: Tropospheric emission spectrometer: Retrieval method and error analysis, IEEE TRANSACTIONS ON GEOSCIENCE AND REMOTE SENSING, 44(5), 1297–1307, 2006.

Connor, B. J., B ̈osch, H., Toon, G., Sen, B., Miller, C., andCrisp, D.: Orbiting Carbon Observatory: Inverse method andprospective error analysis, J. Geophys. Res., 113, A05305,doi:10.1029/2006JD008336, 2008.

Connor, T. C., Shephard, M. W., Payne, V. H., Cady-Pereira, K. E., Kulawik, S. S., Luo, M., Osterman, G., and Lampel, M.: Long-term stability of TES satellite radiance measurements, Atmos. Meas. Tech., 4, 1481–1490, https://doi.org/10.5194/amt-4-1481-2011, 2011

Connor, B., Bösch, H., McDuffie, J., Taylor, T., Fu, D., Frankenberg, C., O'Dell, C., Payne, V. H., Gunson, M., Pollock, R., Hobbs, J., Oyafuso, F., and Jiang, Y.: Quantification of uncertainties in OCO-2 measurements of XCO2: simulations and linear error analysis, Atmos. Meas. Tech., 9, 5227–5238, https://doi.org/10.5194/amt-9-5227-2016, 2016.

Cooperative Global Atmospheric Data Integration Project: Multi-laboratory compilation of atmospheric methane data for the period 1957-2017; obspack_ch4_1_GLOBALVIEWplus_v1.0_2019_01_08; NOAA, Earth System Research Laboratory, Global Monitoring Division, http://dx.doi.org/10.25925/20190108, 2019.

Crevoisier, C., Nobileau, D., Armante, R., Crépeau, L., Machida, T., Sawa, Y., Matsueda, H., Schuck, T., Thonat, T., Pernin, J., Scott, N. A. and Chedin, A.: The 2007–2011 evolution of tropical methane in the mid-troposphere as seen from space by MetOp-A/IASI, Atmospheric Chemistry and Physics, 13(8), 4279–4289, doi:10.5194/acp-13-4279-2013, 2013.

DeSouza-Machado, S., Strow, L. L., Tangborn, A., Huang, X., Chen, X., Liu, X., Wu, W. and Yang, Q.: Single-footprint retrievals for AIRS using a fast TwoSlab cloud-representation model and the SARTA all-sky infrared radiative transfer algorithm, Atmos. Meas. Tech., 11(1), 529–550, doi:10.1029/2005GL023211, 2018.

de Lange, A. and Landgraf, J.: Methane profiles from GOSAT thermal infrared spectra, Atmos. Meas. Tech., 11, 3815–3828, https://doi.org/10.5194/amt-11-3815-2018, 2018

De Wachter, E., Kumps, N., Vandaele, A. C., Langerock, B., and De Mazière, M.: Retrieval and validation of MetOp/IASI methane, Atmos. Meas. Tech., 10, 4623–4638, https://doi.org/10.5194/amt-10-4623-2017, 2017.

Formatted: Normal

Formatted: Font color: Black

Formatted: Normal, Border: Top: (No border), Bottom: (No border), Left: (No border), Right: (No border), Between : (No border), Tab stops: 3.13", Centered + 6.27", Right

Folberth, G. A., Hauglustaine, D. A., Lathière, J., and Brocheton, F., Interactive chemistry in the Laboratoire de Météorologie Dynamique general circulation model: model description and impact analysis of biogenic hydrocarbons on tropospheric chemistry. Atmospheric Chemistry and Physics, 6(8), 2273–2319. https://doi.org/10.5194/acp-6-2273-2006, 2006.

Frankenberg, C., Meirink, J., Van Weele, M., Platt, U. and Wagner, T.: Assessing methane emissions from global space-borne observations, Science, 308(5724), 1010–1014, doi:10.1126/science.1106644, 2005.

Frankenberg, C., Aben, I., Bergamaschi, P., Dlugokencky, E. J., van Hees, R., Houweling, S., van der Meer, P., Snel, R. and Tol, P.: Global column-averaged methane mixing ratios from 2003 to 2009 as derived from SCIAMACHY: Trends and variability, J. Geophys. Res, 116(D4), D04302, doi:10.1029/2010JD014849, 2011.

Fu, D., Worden, J. R., Liu, X., Kulawik, S. S., Bowman, K. W. and Natraj, V.: Characterization of ozone profiles derived from Aura TES and OMI radiances, Atmospheric Chemistry and Physics, 13(6), 3445–3462, doi:10.5194/acp-13-3445-2013, 2013.

Fu, D., Bowman, K. W., Worden, H. M., Natraj, V., Worden, J. R., Yu, S., Veefkind, P., Aben, I., Landgraf, J., Strow, L., and Han, Y.: High-resolution tropospheric carbon monoxide profiles retrieved from CrIS and TROPOMI, Atmos. Meas. Tech., 9, 2567-4572579, https://doi.org/10.5194/amt-9-2567-2016, 2016.

Fu, D., Kulawik, S. S., Miyazaki, K., Bowman, K. W., Worden, J. R., Eldering, A., Livesey, N. J., Teixeira, J., Irion, F. W., Herman, R. L., Osterman, G. B., Liu, X., Levelt, P. F., Thompson, A. M. and Luo, M.: Retrievals of tropospheric ozone profiles from the synergism of AIRS and OMI: methodology and validation, Atmospheric Measurement Techniques, 11(10), 5587–5605, doi:10.5194/amt-11-5587-2018-supplement, 2018.

Fu D., Millet D.B., Wells K.C., Payne V.H., Yu S., Guenther A., and Eldering A.: Direct retrieval of isoprene from satellite-based infrared measurements, Nature Communication, 10.3811, doi:10.1038/s41467-019-11835-0. 2019.

Herman, Robert, Kulawik, S. S., Kevin Bowman, Karen Cady-Pereira, Annmarie Eldering, Brendan Fisher, Dejian Fu, Robert Herman, Daniel Jacob, Line Jourdain, Susan Kulawik, Ming Luo, Ruth Monarrez, Gregory Osterman, Susan Paradise, Vivienne Payne, Sassaneh Poosti, Nigel Richards, David Rider, Douglas Shepard, Mark Shephard, Felicia Vilnrotter, Helen Worden, John Worden, Hyejung Yun, Lin Zhang, Level 2 (L2) Data User's Guide (Up to & including Version 7 data), found at https://tes.jpl.nasa.gov/pdf/TES_Level_2_Data_Users_Guide_V7.0.pdf, 2018.

Hu, H., Landgraf, J., Detmers, R., Borsdorff, T., Aan de Brugh, J., Aben, I., et al. (2018). Toward global mapping of methane with TROPOMI: First results and intersatellite comparison to GOSAT. Geophysical Research Letters, 45, 3682– 3689. https://doi.org/10.1002/2018GL077259

Irion, F. W., Kahn, B. H., Schreier, M. M., Fetzer, E. J., Fishbein, E., Fu, D., Kalmus, P., Wilson, R. C., Wong, S. and Yue, Q.: Single-footprint retrievals of temperature, water vapor and cloud properties from AIRS, Atmos. Meas. Tech., 11(2), 971–995, doi:10.1117/12.615244, 2018.

Kort, E. A., Patra, P. K., Ishijima, K., Daube, B. C., Jiménez, R.,Elkin, J., Hurst, D., Moore, F. L., Sweeney, C., and Wofsy,S. C.: Tropospheric distribution and variability of N2O: Evidencefor strong tropical emissions, Geophys. Res. Lett., 38, L15806,https://doi.org/10.1029/2011GL047612, 2011.

Formatted: Normal

Formatted: Font color: Black

Formatted: Normal, Border: Top: (No border), Bottom: (No border), Left: (No border), Right: (No border), Between : (No border), Tab stops: 3.13", Centered + 6.27", Right

Kort, E. A., Wofsy, S. C., Daube, B. C., Diao, M., Elkins, J. W., Gao, R. S., Hintsa, E. J., Hurst, D. F., Jiménez, R., Moore, F. L., Spackman, J. R. and Zondlo, M. A.: Atmospheric observations of Arctic Ocean methane emissions up to 82° north, Nature Geoscience, 5(5), 318–321, doi:10.1038/ngeo1452, 2012.

Kort, E. A., Frankenberg, C., Costigan, K. R., Lindenmaier, R., dubey, M. K. and Wunch, D.: Four corners: The largest US methane anomaly viewed from space, Geophysical Research Letters, 10, 6898, doi:10.1002/2014GL061503, 2014.

Kulawik, S. S., Worden, H., Osterman, G., Ming Luo, Beer, R., Kinnison, D. E., Bowman, K. W., Worden, J., Eldering, A., Lampel, M., Steck, T. and Rodgers, C. D.: TES atmospheric profile retrieval characterization: an orbit of simulated observations, IEEE TRANSACTIONS ON GEOSCIENCE AND REMOTE SENSING, 44(5), 1324–1333, doi:10.1109/TGRS.2006.871207, 2006a.

Kulawik, S. S., Worden, J., Eldering, A., Bowman, K., Gunson, M., Osterman, G. B., Zhang, L., Clough, S. A., Shephard, M. W. and Beer, R.: Implementation of cloud retrievals for Tropospheric Emission Spectrometer (TES) atmospheric retrievals: part 1. Description and characterization of errors on trace gas retrievals, Journal of Geophysical Research-Atmospheres, 111, D24204, doi:10.1029/2005JD006733, 2006b.

Kulawik, S. S., O'Dell, C., Payne, V. H., Kuai, L., Worden, H. M., Biraud, S. C., Sweeney, C., Stephens, B., Iraci, L. T., Yates, E. L., and Tanaka, T.: Lower-tropospheric CO2 from near-infrared ACOS-GOSAT observations, Atmos. Chem. Phys., 17, 5407–5438, https://doi.org/10.5194/acp-17-5407-2017, 2017.

Maasakkers, J. D., Jacob, D. J., Sulprizio, M. P., Scarpelli, T. R., Nesser, H., Sheng, J.-X., Zhang, Y., Hersher, M., Bloom, A. A., Bowman, K. W., Worden, J. R., Janssens-Maenhout, G., and Parker, R. J.: Global distribution of methane emissions, emission trends, and OH concentrations and trends inferred from an inversion of GOSAT satellite data for 2010–2015, Atmospheric Chemistry and Physics, 19(11), 7859–7881, doi:10.5194/acp-19-7859-2019, 2019.

Molod, A. Takacs, Lawrence, Suarez, Max, Bacmeister, Julio, Song, In-Sun, Eichmann, Andrew. The GEOS-5 atmospheric general circulation model: mean climate and development from MERRA to Fortuna. Tech. Rep. 28, Goddard Space Flight Center, NASA/TM–2012-104606 28, 1–124 (2012). https://ntrs.nasa.gov/search.jsp?R=20120011790.

Moncet, J-L. et al: Algorithm theoretical basis document for the Cross Track Infrared Sound er (CrIS). Volume II, Environmental Data Records (EDR), version 4.2. AER Tech. Doc. P1187-TR-I-08, 298 pp. [Available online at http://npp.gsfc.nasa.gov/sciencedocuments/2013-01/474-00056_RevABaseline.pdf.], 2005

Moncet, J-L., G. Uymin, A. E. Lipton, and H. E. Snell: Infrared radiance modeling by optimal spectral sampling. J. Atmos. Sci., 65, 3917–3934, doi: 10.1175/2008JAS2711.1, 2008

Moncet, J-L., Uymin, G., Liang, P. and Lipton, A.E: Fast and accurate radiative transfer in the thermal regime by simultaneous optimal spectral sampling over all channels. Journal of the Atmospheric Sciences, vol 72, 2622-2641, doi: 0.1175/JAS-D-14-0190.1, 2015

Ostler, A., Sussmann, R., Patra, P. K., Houweling, S., De Bruine, M., Stiller, G. P., Haenel, F. J., Plieninger, J., Bousquet, P., Yin, Y., Saunois, M., Walker, K. A., Deutscher, N. M., Griffith, D. W. T., Blumenstock, T., Hase, F., Warneke, T., Wang, Z.,

Formatted: Normal

Formatted: Font color: Black

Formatted: Normal, Border: Top: (No border), Bottom: (No border), Left: (No border), Right: (No border), Between : (No border), Tab stops: 3.13", Centered + 6.27", Right

Kivi, R., and Robinson, J.: Evaluation of column-averaged methane in models and TCCON with a focus on the stratosphere, Atmos. Meas. Tech., 9, 4843–4859, https://doi.org/10.5194/amt-9-4843-2016, 2016.

Pagano, T. S., Aumann, H. H., Hagan, D. E., and Overoye, K.: Prelaunch and in-flight radiometric calibration of the Atmospheric Infrared Sounder (AIRS), IEEE T. Geosci. Remote, 41, 265–273, 2003.

Parker, R., Boesch, H., Cogan, A., Fraser, A., Feng, L., Palmer, P. I., Messerschmidt, J., Deutscher, N., Griffith, D. W. T., Notholt, J., Wennberg, P. O. and Wunch, D.: Methane observations from the Greenhouse Gases Observing SATellite: Comparison to ground-based TCCON data and model calculations, Geophys. Res. Lett, 38(15), L15807, doi:10.1029/2011GL047871, 2011.

Rigby, M., Montzka, S. A., Prinn, R. G., White, J. W. C., Young, D., O'Doherty, S., Lunt, M. F., Ganesan, A. L., Manning, A. J., Simmonds, P. G., Salameh, P. K., Harth, C. M., Muehle, J., Siddans, R., Knappett, D., Kerridge, B., Waterfall, A., Hurley, J., Latter, B., Boesch, H., and Parker, R.: Global height-resolved methane retrievals from the Infrared Atmospheric Sounding Interferometer (IASI) on MetOp, Atmos. Meas. Tech., 10, 4135–4164, https://doi.org/10.5194/amt-10-4135-2017, 2017.

Pandey, S., Gautam, R., Houweling, S., van der Gon, H. D., Sadavarte, P., Borsdorff, T., Hasekamp, O., Landgraf, J., Tol, P., van Kempen, T., Hoogeveen, R., van Hees, R., Hamburg, S. P., Maasakkers, J. D., and Aben, I.: Satellite observations reveal extreme methane leakage from a natural gas well blowout, Proc Natl Acad Sci USA, 116, 26376-26381, DOI: 10.1073/pnas.1908712116, 2019.

Patra, P. K., Houweling, S., Krol, M., Bousquet, P., Belikov, D., Bergmann, D., Bian, H., Cameron-Smith, P., Chipperfield, M. P., Corbin, K., Fortems-Cheiney, A., Fraser, A., Gloor, E., Hess, P., Ito, A., Kawa, S. R., Law, R. M., Loh, Z., Maksyutov, S., Meng, L., Palmer, P. I., Prinn, R. G., Rigby, M., Saito, R., and Wilson, C.: TransCom model simulations of CH4 and related species: linking transport, surface flux and chemical loss with CH4 variability in the troposphere and lower stratosphere, Atmos. Chem. Phys., 11, 12813–12837, https://doi.org/10.5194/acp-11-12813-2011, 2011.

Razavi, A., Clerbaux, C., Wespes, C., Clarisse, L., Hurtmans, D., Payan, S., Camy-Peyret, C., and Coheur, P. F.: Characterization of methane retrievals from the IASI space-borne sounder, Atmos. Chem. Phys., 9, 7889–7899, https://doi.org/10.5194/acp-9-7889-2009, 2009

Rodgers, C. D.: Inverse Methods for Atmospheric Sounding: The- ory and Practice, World Sci., Tokyo, 2000.

Santoni, G. W., Daube, B. C., Kort, E. A., Jiménez, R., Park, S., Pittman, J. V., Gottlieb, E., Xiang, B., Zahniser, M. S., Nelson, D. D., McManus, J. B., Peischl, J., Ryerson, T. B., Holloway, J. S., Andrews, A. E., Sweeney, C., Hall, B., Hintsa, E. J., Moore, F. L., Elkins, J. W., Hurst, D. F., Stephens, B. B., Bent, J., and Wofsy, S. C.: Evaluation of the airborne quantum cascade laser spectrometer (QCLS) measurements of the carbon and greenhouse gas suite – CO2, CH4, N2O, and CO – during the CalNex and HIPPO campaigns, Atmos. Meas. Tech., 7, 1509–1526, https://doi.org/10.5194/amt-7-1509-2014, 2014.

Schepers, D., Guerlet, S., Butz, A., Landgraf, J., Frankenberg, C., Hasekamp, O., Blavier, J.-F., Deutscher, N. M., Griffith, D. W. T., Hase, F., Kyro, E., Morino, I., Sherlock, V., Sussmann, R., and Aben, I.: Methane retrievals from Greenhouse Gases Observing Satellite (GOSAT) shortwave infrared measurements: performance comparison of proxy and physics retrieval algorithms, J. Geophys. Res., 117, D10307, doi:10.1029/2012JD017549, 2012.

Formatted: Normal

Formatted: Not Superscript/ Subscript

Formatted: Not Superscript/ Subscript

Formatted: Not Superscript/ Subscript

Formatted: Not Superscript/ Subscript

Formatted: Not Superscript/ Subscript

Formatted: Font color: Black

Formatted: Normal, Border: Top: (No border), Bottom: (No border), Left: (No border), Right: (No border), Between : (No border), Tab stops: 3.13", Centered + 6.27", Right

Shephard, M.W., Worden, H.M., Cady-Pereira, K.E., Lampel, M., Luo, M., Bowman, K.W., Sarkissian, E., Beer, R., Rider, D.M., Tobin, D.C., Revercomb, H.E., Fisher, B.M., Tremblay, D., Clough, S.A., Osterman, G.B., and Gunson, M., Tropospheric Emission Spectrometer nadir spectral radiance comparisons, J. Geophys. Res., 113, D15S05, doi:10.1029/2007JD008856, 2008.

Siddans, R., Knappett, D., Kerridge, B., Waterfall, A., Hurley, J., Latter, B., Boesch, H., and Parker, R.: Global height-resolved methane retrievals from the Infrared Atmospheric Sounding Interferometer (IASI) on MetOp, Atmos. Meas. Tech., 10, 4135–4164, https://doi.org/10.5194/amt-10-4135-2017, 2017.

Smith, N. and Barnet, C. D. (2019), Uncertainty characterization and propagation in the Community Long-Term Infrared Microwave Combined Atmospheric Product System (CLIMCAPS), Remote Sens., 11, doi:10.3390/rs11101227

Turner, A. J., Frankenberg, C. and Kort, E. A.: Interpreting contemporary trends in atmospheric methane, Proceedings of the National Academy of Sciences of the United States of America, 8(8), 201814297–9, doi:10.1073/pnas.1814297116, 2019.

Turner, A. J., Fung, I., Naik, V., Horowitz, L. W. and Cohen, R. C.: Modulation of hydroxyl variability by ENSO in the absence of external forcing, Proceedings of the National Academy of Sciences of the United States of America, 115(36), 8931–8936, doi:10.1073/pnas.1807532115, 2018a.

Turner, A. J., Jacob, D. J., Benmergui, J., Brandman, J., White, L. and Randles, C. A.: Assessing the capability of different satellite observing configurations to resolve the distribution of methane emissions at kilometer scales, Atmospheric Chemistry and Physics, 18(11), 8265–8278, doi:10.5194/acp-18-8265-2018, 2018b.

Turner, A.J., D.J. Jacob, K.J. Wecht, J.D. Maasakkers, E. Lundgren, A.E. Andrews, S.C. Biraud, H. Boesch, K.W. Bowman, N.M. Deutscher, M.K. Dubey, D.W.T. Griffith, F. Hase, A. Kuze, J. Notholt, H. Ohyama, R. Parker, V.H. Payne, R. Sussmann, C. Sweeney, V.A. Velazco, T. Warneke, P.O. Wennberg, and D. Wunch Estimating global and North American methane emissions with high spatial resolution using GOSAT satellite data, Atmos. Chem. Phys., 15, 7049-7069, 2015.

Varon, D. J., McKeever, J., Jervis, D., Maasakkers, J. D., Pandey, S., Houweling, S., et al. (2019). Satellite discovery of anomalously large methane point sources from oil/gas production. Geophysical Research Letters, 46, 13507– 13516. https://doi.org/10.1029/2019GL083798

Wecht, K. J., Jacob, D. J., Wofsy, S. C., Kort, E. A., Worden, J. R., Kulawik, S. S., Henze, D. K., Kopacz, M. and Payne, V. H.: Validation of TES methane with HIPPO aircraft observations: implications for inverse modeling of methane sources, Atmospheric Chemistry and Physics, 12(4), 1823–1832, doi:10.5194/acp-12-1823-2012, 2012.

Wecht, K. J., Jacob, D. J. and Sulprizio, M. P.: Spatially resolving methane emissions in California: constraints from the CalNex aircraft campaign and from present (GOSAT, TES) and future (TROPOMI) missions, Atmospheric Chemistry and Physics, doi:10.5194/acp-14-8173-2014, 2014.

Wofsy, S. C., B. C. Daube, R. Jimenez, E. Kort, J. V. Pittman, S. Park, R. Commane, B. Xiang G. Santoni, D. Jacob, J. Fisher, C. Pickett-Heaps, H. Wang, K. Wecht, Q.-Q. Wang, B. B. Stephens, S. Shertz, A.S. Watt, P. Romashkin, T. Campos, J. Haggerty, W. A. Cooper, D. Rogers, S. Beaton, R. Hendershot, J. W. Elkins, D. W. Fahey, R. S. Gao, F. Moore, S. A. Montzka, J. P. Schwarz, A. E. Perring, D. Hurst, B. R. Miller, C. Sweeney, S. Oltmans, D. Nance, E. Hintsa, G. Dutton, L. A. Watts, J.

Formatted: Normal

Formatted: Font color: Black

Formatted: Normal, Border: Top: (No border), Bottom: (No border), Left: (No border), Right: (No border), Between : (No border), Tab stops: 3.13", Centered + 6.27", Right

R. Spackman, K. H. Rosenlof, E. A. Ray, B. Hall, M. A. Zondlo, M. Diao, R. Keeling, J. Bent, E. L. Atlas, R. Lueb, M. J. Mahoney. HIPPO Merged 10-second Meteorology, Atmospheric Chemistry Aerosol Data (R_20121129), Carbon Dioxide Information Analysis Center, Oak Ridge National Laboratory, Oak Ridge, Tennessee U.S.A., 2012.

Wofsy, S.C., ~~and ATom Science Team. ATom: Aircraft Flight Track and Navigational Data. ORNL DAAC, Oak Ridge, Tennessee, USA, 2018. https://doi.org/10.3334/ORNLDAAC/1613~~S. Afshar, H.M. Allen, E.C. Apel, E.C. Asher, B. Barletta, J. Bent, H. Bian, B.C. Biggs, D.R. Blake, N. Blake, I. Bourgeois, C.A. Brock, W.H. Brune, J.W. Budney, T.P. Bui, A. Butler, P. Campuzano-Jost, C.S. Chang, M. Chin, R. Commane, G. Correa, J.D. Crounse, P. D. Cullis, B.C. Daube, D.A. Day, J.M. Dean-Day, J.E. Dibb, J.P. DiGangi, G.S. Diskin, M. Dollner, J.W. Elkins, F. Erdesz, A.M. Fiore, C.M. Flynn, K.D. Froyd, D.W. Gesler, S.R. Hall, T.F. Hanisco, R.A. Hannun, A.J. Hills, E.J. Hintsa, A. Hoffman, R.S. Hornbrook, L.G. Huey, S. Hughes, J.L. Jimenez, B.J. Johnson, J.M. Katich, R.F. Keeling, M.J. Kim, A. Kupc, L.R. Lait, J.-F. Lamarque, J. Liu, K. McKain, R.J. Mclaughlin, S. Meinardi, D.O. Miller, S.A. Montzka, F.L. Moore, E.J. Morgan, D.M. Murphy, L.T. Murray, B.A. Nault, J.A. Neuman, P.A. Newman, J.M. Nicely, X. Pan, W. Paplawsky, J. Peischl, M.J. Prather, D.J. Price, E. Ray, J.M. Reeves, M. Richardson, A.W. Rollins, K.H. Rosenlof, T.B. Ryerson, E. Scheuer, G.P. Schill, J.C. Schroder, J.P. Schwarz, J.M. St.Clair, S.D. Steenrod, B.B. Stephens, S.A. Strode, C. Sweeney, D. Tanner, A.P. Teng, A.B. Thames, C.R. Thompson, K. Ullmann, P.R. Veres, N. Vieznor, N.L. Wagner, A. Watt, R. Weber, B. Weinzierl, P.O. Wennberg, C.J. Williamson, J.C. Wilson, G.M. Wolfe, C.T. Woods, and L.H. Zeng. 2018. ATom: Merged Atmospheric Chemistry, Trace Gases, and Aerosols. ORNL DAAC, Oak Ridge, Tennessee, USA. https://doi.org/10.3334/ORNLDAAC/1581

Worden, J., Kulawik, S., Shepard, M., Clough, S., Worden, H., Bowman, K. and Goldman, A.: Predicted errors of tropospheric emission spectrometer nadir retrievals from spectral window selection, Journal of Geophysical Research-Atmospheres, 109(D9), D09308, doi:10.1029/2004JD004522, 2004.

Worden, J., Noone, D., Galewsky, J., Bailey, A., Bowman, K., Brown, D., Hurley, J., Kulawik, S., Lee, J. and Strong, M.: Estimate of bias in Aura TES HDO/H2O profiles from comparison of TES and in situ HDO/H2O measurements at the Mauna Loa observatory, Atmospheric Chemistry and Physics, 11(9), 4491–4503, doi:10.5194/acp-11-4491-2011, 2011.

Worden, J., Kulawik, S., Frankenberg, C., Payne, V., Bowman, K., Cady-Peirara, K., Wecht, K., Lee, J.-E., and Noone, D.: Profiles of CH4, HDO, H2O, and N2O with improved lower tropospheric vertical resolution from Aura TES radiances, Atmos. Meas. Tech., 5, 397-411, https://doi.org/10.5194/amt-5-397-2012, 2012.

Worden, J., K. Wecht, C. Frankenberg, M. Alvarado, K. Bowman, E. Kort, S. Kulawik, M. Lee, V. Payne, and H. Worden, CH4 and CO distributions over tropical fires during October 2006 observed by the Aura TES satellite instrument and modeled by GEOS-Chem, Atmospheric Chemistry and Physics, 13(7), 3679–3692, doi:10.5194/acp-13-3679-2013, 2013a.

Worden, J., Jiang, Z., Jones, D. B. A., Alvarado, M., Bowman, K., Frankenberg, C., Kort, E. A., Kulawik, S. S., Lee, M., Liu, J., Payne, V., Wecht, K. and Worden, H.: El Nino, the 2006 Indonesian Peat Fires, and the distribution of atmospheric methane, Geophys. Res. Lett, 40, 1, doi:10.1002/grl.50937, 2013b.

Formatted: Normal

Formatted: Not Superscript/ Subscript

Formatted: Not Superscript/ Subscript

Formatted: Not Superscript/ Subscript

Formatted: Not Superscript/ Subscript

Formatted: Font color: Black

Formatted: Normal, Border: Top: (No border), Bottom: (No border), Left: (No border), Right: (No border), Between : (No border), Tab stops: 3.13", Centered + 6.27", Right

Worden, J. R., Turner, A. J., Bloom, A., Kulawik, S. S., Liu, J., Lee, M., Weidner, R., Bowman, K., Frankenberg, C., Parker, R., and Payne, V. H.: Quantifying lower tropospheric methane concentrations using GOSAT near-IR and TES thermal IR measurements, Atmos. Meas. Tech., 8, 3433-3445, https://doi.org/10.5194/amt-8-3433-2015, 2015.

Worden, J. R., Bloom, A. A., Pandey, S., Jiang, Z., Worden, H. M., Walker, T. W., Houweling, S. and Röckmann, T.: Reduced biomass burning emissions reconcile conflicting estimates of the post-2006 atmospheric methane budget, Nat Commun, 1–11, doi:10.1038/s41467-017-02246-0, 2017a.

Worden, J. R., Doran, G., Kulawik, S., Eldering, A., Crisp, D., Frankenberg, C., O amp apos Dell, C. and Bowman, K.: Evaluation and attribution of OCO-2 XCO2 uncertainties, Atmospheric Measurement Techniques, 10(7), 2759–2771, doi:10.5194/amt-10-2759-2017, 2017b.

Worden, J. R., Kulawik, S. S., Fu, D., Payne, V. H., Lipton, A. E., Polonsky, I., He, Y., Cady-Pereira, K., Moncet, J.-L., Herman, R. L., Irion, F. W. and Bowman, K. W.: Characterization and evaluation of AIRS-based estimates of the deuterium content of water vapor, Atmospheric Measurement Techniques, 12(4), 2331–2339, doi:10.5194/amt-12-2331-2019, 2019.

Wunch, D., Toon, G. C., Wennberg, P. O., Wofsy, S. C., Stephens, B. B., Fischer, M. L., Uchino, O., Abshire, J. B., Bernath, P., Biraud, S. C., Blavier, J.-F. L., Boone, C., Bowman, K. P., Browell, E. V., Campos, T., Connor, B. J., Daube, B. C., Deutscher, N. M., Diao, M., Elkins, J. W., Gerbig, C., Gottlieb, E., Griffith, D. W. T., Hurst, D. F., Jiménez, R., Keppel-Aleks, G., Kort, E. A., Macatangay, R., Machida, T., Matsueda, H., Moore, F., Morino, I., Park, S., Robinson, J., Roehl, C. M., Sawa, Y., Sherlock, V., Sweeney, C., Tanaka, T., and Zondlo, M. A.: Calibration of the Total Carbon Column Observing Network using aircraft profile data, Atmos. Meas. Tech., 3, 1351–1362, https://doi.org/10.5194/amt-3-1351-2010, 2010.

Xiong, X., Barnet, C., Maddy, E., Wofsy, S. C., Chen, L. A., Karion, A. and Sweeney, C.: Detection of methane depletion associated with stratospheric intrusion by atmospheric infrared sounder (AIRS), Geophysical Research Letters, 40(10), 2455–2459, doi:10.1002/grl.50476, 2013.

Xiong, X., Houweling, S., Wei, J., Maddy, E., Sun, F. and Barnet, C.: Methane plume over south Asia during the monsoon season: satellite observation and model simulation, Atmospheric Chemistry and Physics, 9(3), 783–794, 2009.

Xiong X, Han Y, Liu Q and Weng F, Comparison of atmospheric methane retrievals from AIRS and IASI IEEE J. Sel. Top. Appl. Earth Obs. Remote Sens. 9 3297–303, 2016.

Xiong, X., Weng, F., Liu, Q., and Olsen, E.: Space-borne observation of methane from atmospheric infrared sounder version 6: validation and implications for data analysis, Atmos. Meas. Tech. Discuss., 8, 8563–8597, https://doi.org/10.5194/amtd-8-8563-2015, 2015.

Zhang, Y., Jacob, D. J., Maasakkers, J. D., Sulprizio, M. P., Sheng, J.-X., Gautam, R. and Worden, J.: Monitoring global tropospheric OH concentrations using satellite observations of atmospheric methane, Atmospheric Chemistry and Physics, 18(21), 15959–15973, doi:10.1029/2007JG000500, 2018.

Formatted: Normal

Formatted: Font color: Black

Formatted: Normal, Border: Top: (No border), Bottom: (No border), Left: (No border), Right: (No border), Between : (No border), Tab stops: 3.13", Centered + 6.27", Right

Table 1. Bias versus pressure with and without bias correction. The bias correction was developed on HIPPO-4 and tested on HIPPO-4; HIPPO-1,2,3,5; and NOAA aircraft network.

Pressure (hPa)	AIRS minus aircraft_AK (HIPPO-4) (ppb)	After bias correction (HIPPO-4) (ppb)	After bias correction (all HIPPO except HIPPO-4) (ppb)	After bias correction (all NOAA) (ppb)
1000	24	-1	-3	1
824	36	0	-4	1
681	48	1	-5	2
562	58	1	-4	2
464	60	-5	-3	3
383	67	-5	-2	2
316	81	1	4	-
261	86	1	4	-
215	89	1	3	-
161	-	-	4	-

Formatted: Normal

Formatted Table

Formatted: Font: 10 pt

Formatted: Font color: Black

Formatted: Normal, Border: Top: (No border), Bottom: (No border), Left: (No border), Right: (No border), Between : (No border), Tab stops: 3.13", Centered + 6.27", Right

Table A.1 Bias by campaign, station, land/ocean, and pressure.

Station/campaign	Location	Time period	Bias 700 hPa (ppb)	Bias 500 hPa (ppb)	Bias 300 hPa (ppb)	Bias column matching aircraft (ppb)	Bias column above 750 hPa (ppb)
HIPPO 1S	Pacific	Jan, 2009	-6.2	2.4	11.0	4.2	6.3
HIPPO 1N	Pacific	Jan, 2009	-3.2	3.7	12.5	-0.1	4.8
HIPPO 2S	Pacific	Nov, 2009	-9.0	-0.4	9.8	-4.4	5.0
HIPPO 2N	Pacific	Nov, 2009	-4.3	-3.3	-3.1	-4.0	-4.0
HIPPO 3N	Pacific	Apr, 2010	-8.5	1.1	16.5	-2.6	2.6
HIPPO 4S	Pacific	Jun, 2011	-0.7	-2.0	9.5	1.8	10.2
HIPPO 4N	Pacific	Jul, 2011	8.7	11.8	0.7	8.7	7.3
HIPPO 5S	Pacific	Aug, 2011	1.2	7.6	13.3	4.5	9.3
HIPPO 5N	Pacific	Sep, 2011	-5.2	0.5	1.2	-2.0	2.2
HIPPO all land	**-**	**-**	**10.9**	**18.2**	**17.8**	**16.1**	**14.8**
HIPPO all ocean	**-**	**-**	**-5.2**	**-0.9**	**4.3**	**-1.7**	**3.1**
HIPPO all (mean)	**-**	**-**	**-2.9**	**2.1**	**7.9**	**0.7**	**4.9**
HIPPO all (stdev)	**-**	**-**	**5.9**	**5.2**	**6.7**	**4.4**	**4.3**
ACG	68N, 152W	-	21.4	-	-	18.6	26.7
ESP	49N, 126W	-	9.7	-	-	8.2	13.8
NHA	43N, 71W	-	15.7	23.8	-	15.7	19.3
THD	41N, 124W	-	13.6	21.7	-	14.0	21.2
CMA	39N, 74W	-	-0.2	5.7	-	0.9	3.6
TGC	28N, 97W	-	1.0	7.9	-	2.3	6.5
RTA	21S, 160W	-	3.7	11.5	-	3.9	12.8

Formatted: Normal

Formatted Table

Formatted: Font color: Black

Formatted: Normal, Border: Top: (No border), Bottom: (No border), Left: (No border), Right: (No border), Between : (No border), Tab stops: 3.13", Centered + 6.27", Right

~~ESRL~~NOAA all land	**-**	**-**	**9.2**	**16.8**	**-**	**9.4**	**14.3**
~~ESRL~~NOAA all ocean	**-**	**-**	**9.0**	**12.8**	**-**	**8.7**	**15.4**
~~ESRL~~NOAA all (mean)	**-**	**-**	**9.3**	**14.1**	**-**	**9.1**	**14.8**
~~ESRL~~NOAA all (stdev)	**-**	**-**	**8.1**	**8.2**	**-**	**7.1**	**8.2**
ATom 1S	Pacific	Aug, 2016	-0.2	4.5	7.7	2.0	3.5
ATom 1N	Atlantic	Aug, 2016	0.2	3.2	13.2	2.8	6.9
ATom 2S	Pacific	Feb, 2017	-6.8	0.7	8.4	-2.5	5.2
ATom 2N	Atlantic	Feb, 2017	5.7	12.3	25.3	8.3	12.5
ATom 3S	Pacific	Oct, 2017	-2.5	3.0	9.1	0.9	5.9
ATom 3N	Atlantic/Pacific	Oct, 2017	6.5	13.0	21.9	9.3	13.8
ATom 4S	Pacific	April/May, 2018	-0.1	3.9	9.4	2.3	6.0
ATom 4N	Atlantic	May, 2018	-1.4	5.9	23.4	3.4	13.2
ATom all land	**-**	**-**	**16.7**	**23.6**	**26.2**	**17.0**	**18.2**
ATom all ocean	**-**	**-**	**-3.2**	**2.4**	**13.4**	**0.6**	**6.5**
ATom all (mean)	**-**	**-**	**0.1**	**5.8**	**14.7**	**3.2**	**8.3**
ATom all (stdev)	**-**	**-**	**4.3**	**4.5**	**7.5**	**3.8**	**4.1**

Formatted: Normal

Formatted: Font: 10 pt

Formatted: Font color: Black

Formatted: Normal, Border: Top: (No border), Bottom: (No border), Left: (No border), Right: (No border), Between : (No border), Tab stops: 3.13", Centered + 6.27", Right

Table A.2 Change in the mean bias of the partial column matching the ~~aircraft~~NOAAaircraft observation using different aircraft profile extensions from the top aircraft measurement to the top of the atmosphere.

Quantity	Profile extension	Bias 700 hPa (ppb)	Bias 500 hPa (ppb)	Bias 300 hPa (ppb)	Bias column matching aircraft (ppb)	Bias column above 750 hPa (ppb)
Land ~~ESRL~~NOAA	CT	6.0	10.3	-	6.1	3.8
Ocean ~~ESRL~~NOAA	CT	4.5	5.7	-	4.3	4.0
Land ~~ESRL~~NOAA	prior	9.2	16.8	-	9.4	14.3
Ocean ~~ESRL~~NOAA	prior	9.0	12.8	-	8.7	15.4
Land ~~ESRL~~NOAA	GEOS-Chem	6.4	11.7	-	6.7	6.4
Ocean ~~ESRL~~NOAA	GEOS-Chem	4~~.~~.4	7.7	-	4.5	6.4

Formatted: Normal

Formatted Table

Formatted: Font: 10 pt

Formatted: Font color: Black

Formatted: Normal, Border: Top: (No border), Bottom: (No border), Left: (No border), Right: (No border), Between : (No border), Tab stops: 3.13", Centered + 6.27", Right

Table A.3 Standard deviation of AIRS minus validation for land / ocean observations and different pressures / pressure ranges. Rows 1-2 show the standard deviation for single observation, rows 3-4 show the predicted observation error, rows 5-8 show the standard deviation for daily averages, rows 9-10 show the predicted error for daily averages (assuming random error), rows 11-12 show the standard deviation for 3-month averages, rows 13-14 show the standard deviation for seasonal cycle averages (average the same month of all years), rows 15-16 show the predicted error for the seasonal cycle averages, and rows 17-18 show the standard deviation without bias subtraction. The site-dependent biases from Table A.1 are subtracted prior to calculating the standard deviation.

Quantity	Stdev 700 hPa (ppb)	Stdev 500 hPa (ppb)	Stdev 300 hPa (ppb)	**Stdev column matching aircraft (ppb)**	Stdev column above 750 hPa (ppb)
Land single	26	29	26	**23**	25
Ocean single	25	27	26	**22**	24
Land observation error	26	26	19	**23**	19
Ocean observation error	28	28	20	**24**	19
Land daily (≥3 obs/day)	17	21	16	**15**	20
Ocean daily (≥3 obs/day)	18	21	21	**16**	20
Land daily (≥9 obs/day)	16	20	16	**14**	20
Ocean daily (≥9 obs/day)	17	19	21	**15**	18
Land daily (≥9 obs/day) pred.	9.7	9.9	5.7	**8.5**	7.0
Ocean daily (≥9 obs/day) pred.	8.4	7.9	4.6	**7.0**	5.7
Land 3-month (≥3 obs/day, ≥3 days)	9.5	13.3	-	**8.8**	12.9

Formatted: Normal
Formatted Table
Formatted: Font: Gungsuh
Formatted: Font: Gungsuh
Formatted: Font: Gungsuh
Formatted: Font: Gungsuh
Formatted: Font: Gungsuh
Formatted: Font: Gungsuh
Formatted: Font: Gungsuh
Formatted: Font color: Black
Formatted: Normal, Border: Top: (No border), Bottom: (No border), Left: (No border), Right: (No border), Between : (No border), Tab stops: 3.13", Centered + 6.27", Right

Ocean 3-month (≥3 obs/day, ≥ 3 days)	9.0	11.8	-	**8.3**	11.8
Land monthly (average all years)	8.3	11.8	-	**7.7**	10.7
Ocean monthly (average all years)	8.3	10.4	-	**7.5**	10.1
Land monthly (average all years) pred.	7.7	9.9	-	**6.9**	9.3
Ocean monthly (average all years) pred.	8.0	9.8	-	**7.2**	9.5
Land monthly (average all years) without bias subtraction	9.9	13.7	-	**9.1**	12.2
Ocean monthly (average all years) without bias subtraction	10.4	12.3	-	**9.4**	11.6

Formatted: Normal

Formatted: Font: Gungsuh

Formatted: Font color: Black

Formatted: Normal, Border: Top: (No border), Bottom: (No border), Left: (No border), Right: (No border), Between : (No border), Tab stops: 3.13", Centered + 6.27", Right

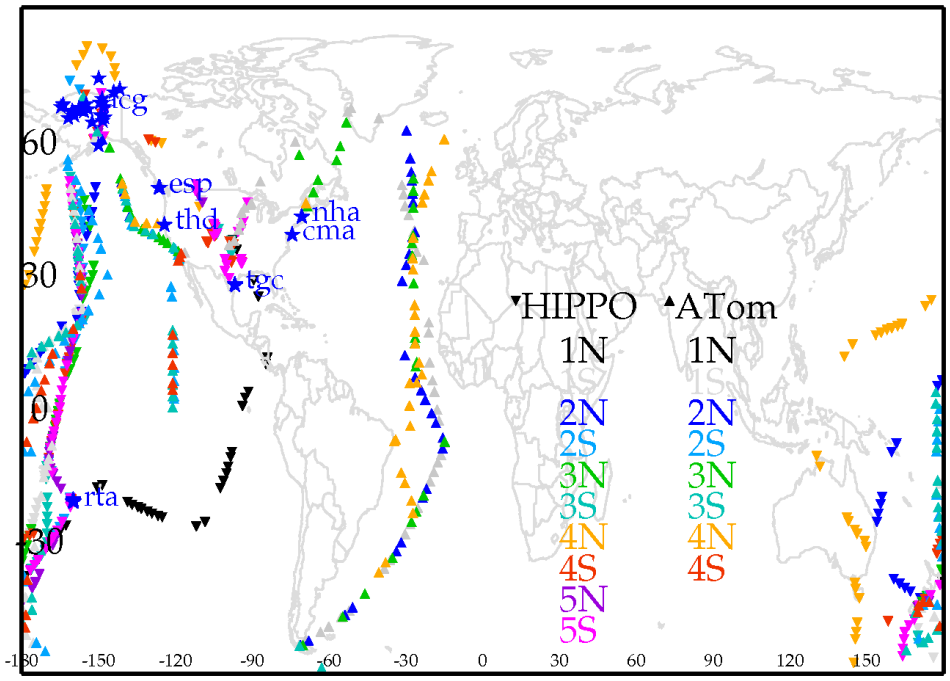

Formatted: Normal

Formatted: Font color: Black

Formatted: Normal, Border: Top: (No border), Bottom: (No border), Left: (No border), Right: (No border), Between : (No border), Tab stops: 3.13", Centered + 6.27", Right

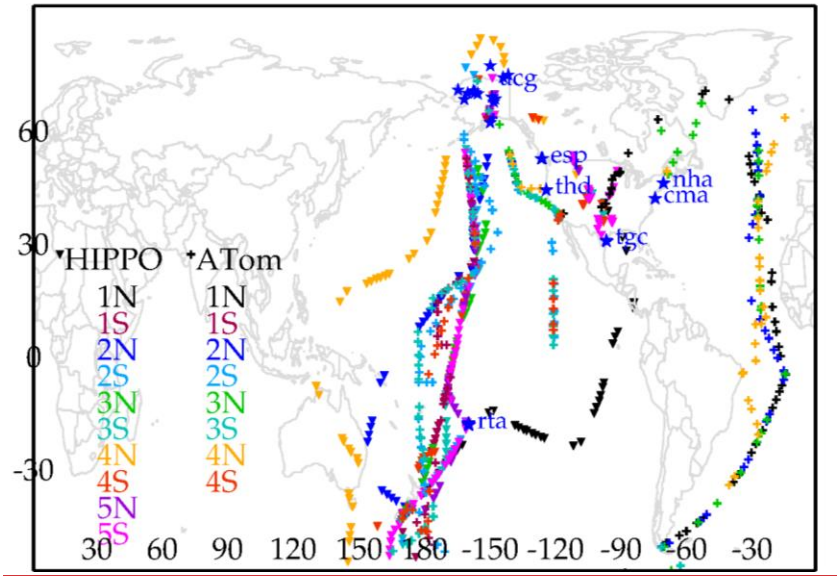

Figure 1: Location of aircraft profile measurements used for validation. The upside-down triangles show HIPPO, ~~triangles+~~ show ATom, and blue stars show NOAA ESRL aircraft validation locations.

Formatted: Normal

Formatted: Font: 9 pt, Bold, Font color: Black

Formatted: Normal, Space After: 10 pt, Border: Top: (No border), Bottom: (No border), Left: (No border), Right: (No border), Between : (No border)

Formatted: Font: 9 pt, Bold, Font color: Black

Formatted: Font color: Black

Formatted: Font color: Black

Formatted: Normal, Border: Top: (No border), Bottom: (No border), Left: (No border), Right: (No border), Between : (No border), Tab stops: 3.13", Centered + 6.27", Right

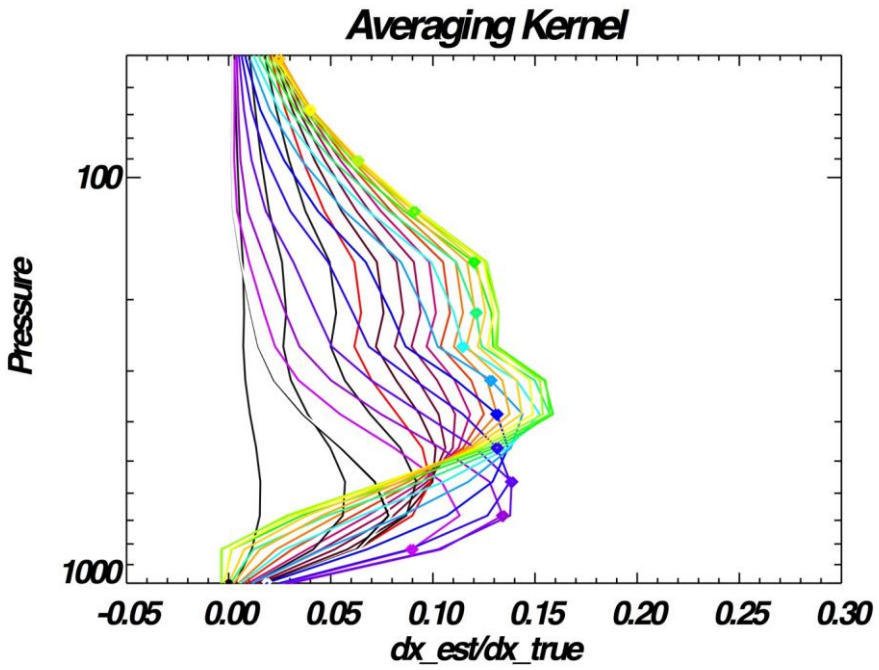

Formatted: Normal

Formatted: Font color: Black

Formatted: Normal, Border: Top: (No border), Bottom: (No border), Left: (No border), Right: (No border), Between : (No border), Tab stops: 3.13", Centered + 6.27", Right

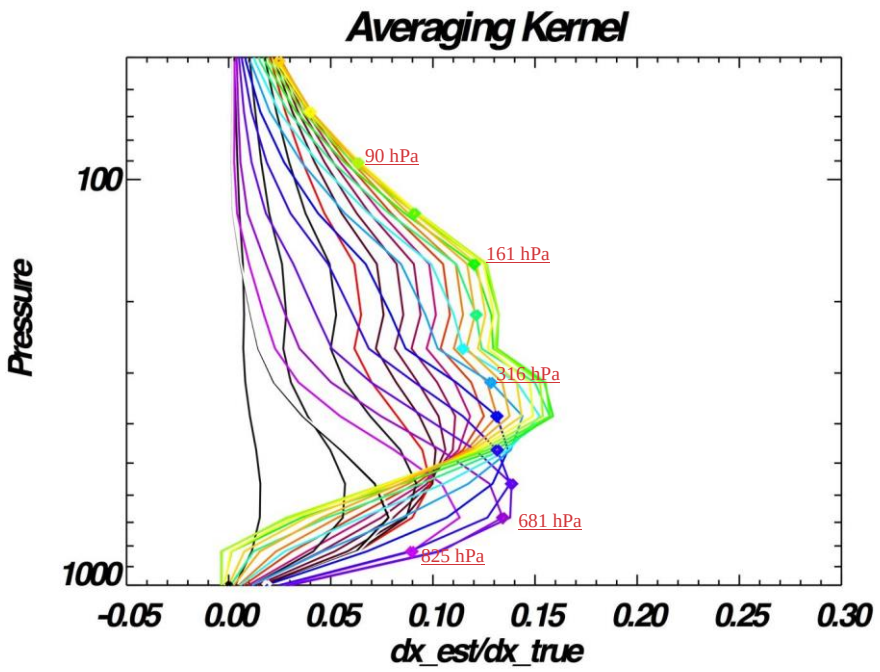

Figure 2: The rows of an averaging kernel for CH_4 for a tropical scene. The colors help for visualization of the pressure levels for each row of the averaging kernel. The diamonds indicate the pressure level corresponding to the row of the averaging kernel, for pressures 1012, 825, 681, 562, 464, 383, 316, 261, 215, 161, 121, 90, 68, 51 hPa.

Formatted: Normal

Formatted: Font: 9 pt, Bold, Font color: Black

Formatted: Normal, Space After: 10 pt, Border: Top: (No border), Bottom: (No border), Left: (No border), Right: (No border), Between : (No border)

Formatted: Font: 9 pt, Bold

Formatted: Font: 9 pt, Bold

Formatted: Font color: Black

Formatted: Font color: Black

Formatted: Normal, Border: Top: (No border), Bottom: (No border), Left: (No border), Right: (No border), Between : (No border), Tab stops: 3.13", Centered + 6.27", Right

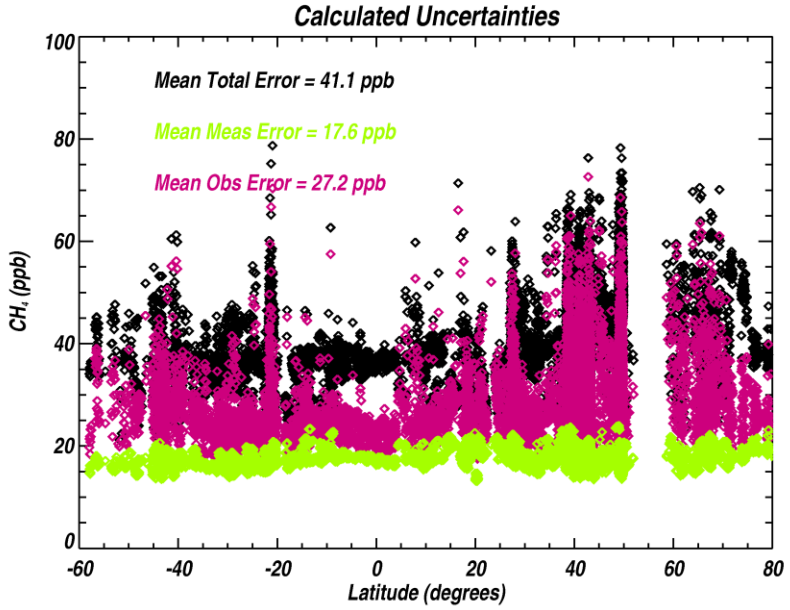

Formatted: Normal

Formatted: Font color: Black

Formatted: Normal, Border: Top: (No border), Bottom: (No border), Left: (No border), Right: (No border), Between : (No border), Tab stops: 3.13", Centered + 6.27", Right

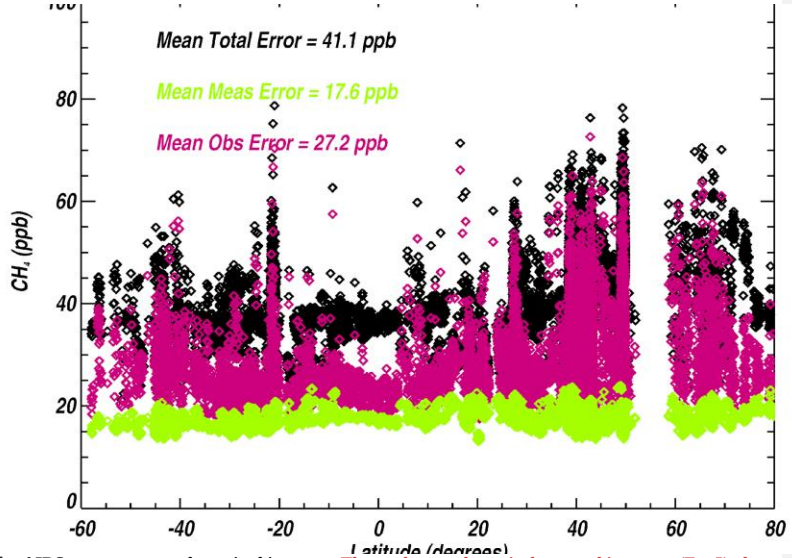

Figure 3: Calculated errors for AIRS measurements shown in this paper. The total error shown is the smoothing error (Eq. 5) plus the observation error (Eq. 7b). The measurement error is the last term of Eq. 7b, and the only fully random error.

Formatted: Normal

Formatted: Font: 9 pt, Bold, Font color: Black

Formatted: Normal, Space After: 10 pt, Border: Top: (No border), Bottom: (No border), Left: (No border), Right: (No border), Between : (No border)

Formatted: Font color: Black

Formatted: Font color: Black

Formatted: Normal, Border: Top: (No border), Bottom: (No border), Left: (No border), Right: (No border), Between : (No border), Tab stops: 3.13", Centered + 6.27", Right

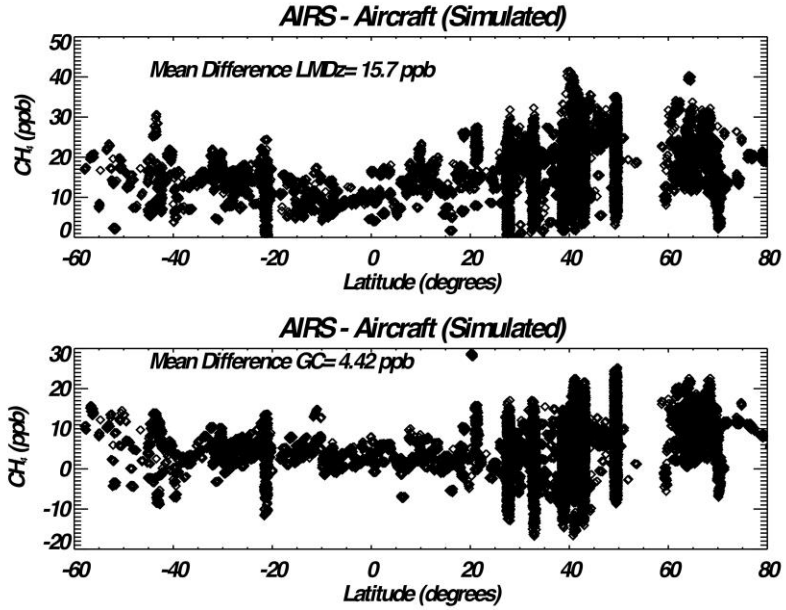

Formatted: Normal

Formatted: Normal, Space After: 10 pt, Border: Top: (No border), Bottom: (No border), Left: (No border), Right: (No border), Between : (No border)

Formatted: Font color: Black

Formatted: Normal, Border: Top: (No border), Bottom: (No border), Left: (No border), Right: (No border), Between : (No border), Tab stops: 3.13", Centered + 6.27", Right

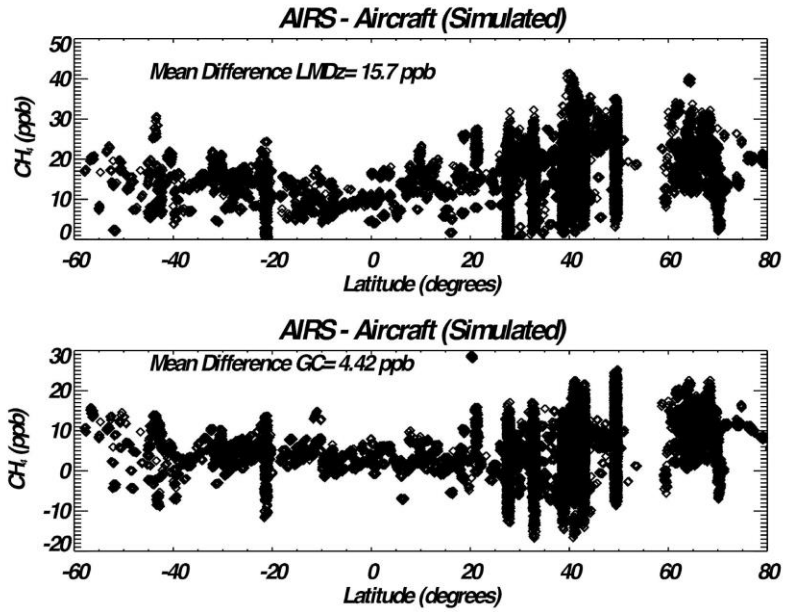

Figure 4: Simulated comparison between AIRS and Aircraft in which the LMDz model (top) and GEOS-Chem model (bottom) are used for the simulation. This represents uncertainty in the true state that we validate against.

Formatted: Normal

Formatted: Font: 9 pt, Bold, Font color: Black

Formatted: Font color: Black

Formatted: Font color: Black

Formatted: Normal, Border: Top: (No border), Bottom: (No border), Left: (No border), Right: (No border), Between : (No border), Tab stops: 3.13", Centered + 6.27", Right

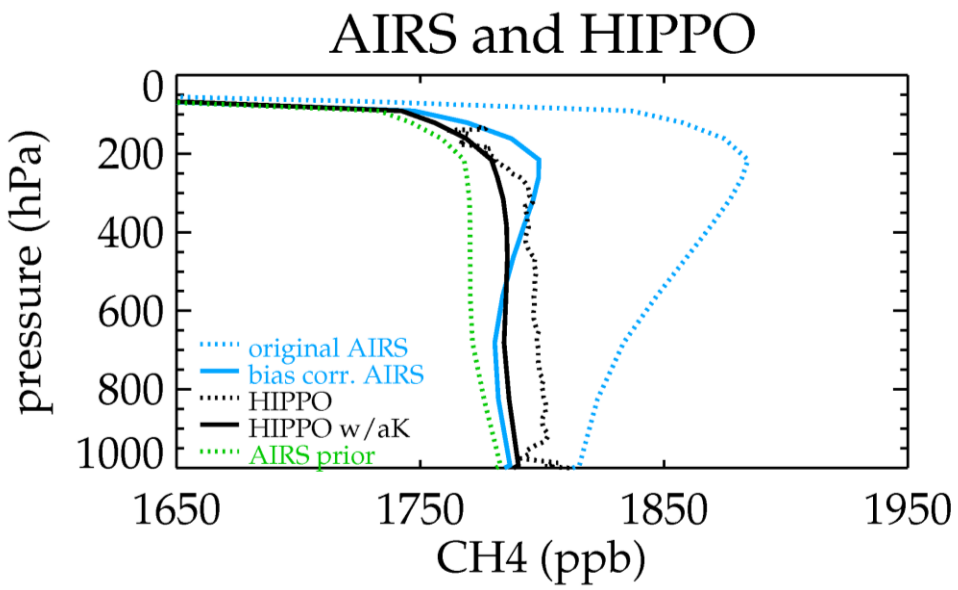

~~Figure 5~~

Formatted: Normal

Formatted: Font color: Black

Formatted: Normal, Border: Top: (No border), Bottom: (No border), Left: (No border), Right: (No border), Between : (No border), Tab stops: 3.13", Centered + 6.27", Right

versus HIPPO observations (no bias correction)

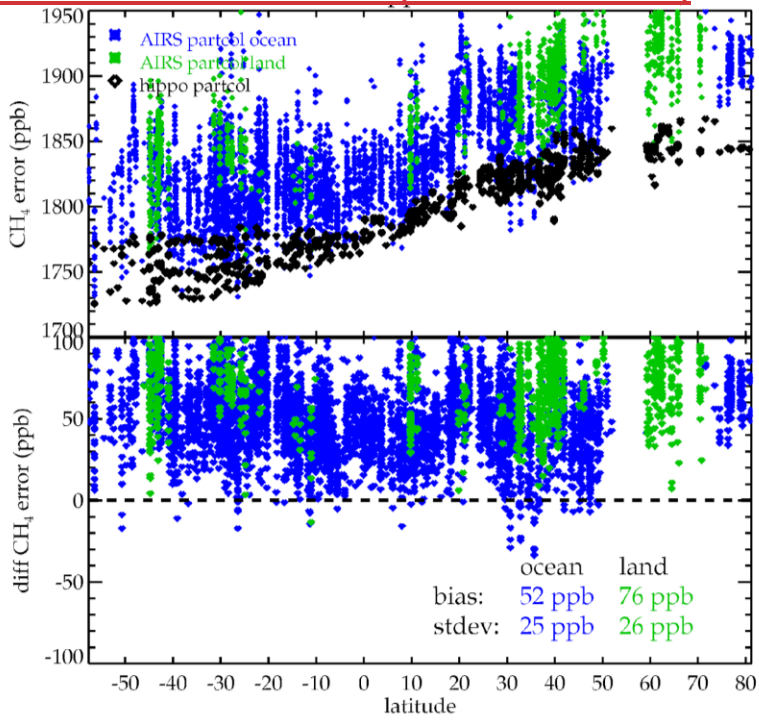

Figure 5: Comparison of AIRS methane VMR to aircraft for all HIPPO comparisons over the partial column XCH_4 VMR within the pressure levels measured by the aircraft. Blue shows AIRS ocean observations and green shows AIRS land observations.

Formatted: Normal

Formatted: Font color: Black

Formatted: Normal, Border: Top: (No border), Bottom: (No border), Left: (No border), Right: (No border), Between : (No border), Tab stops: 3.13", Centered + 6.27", Right

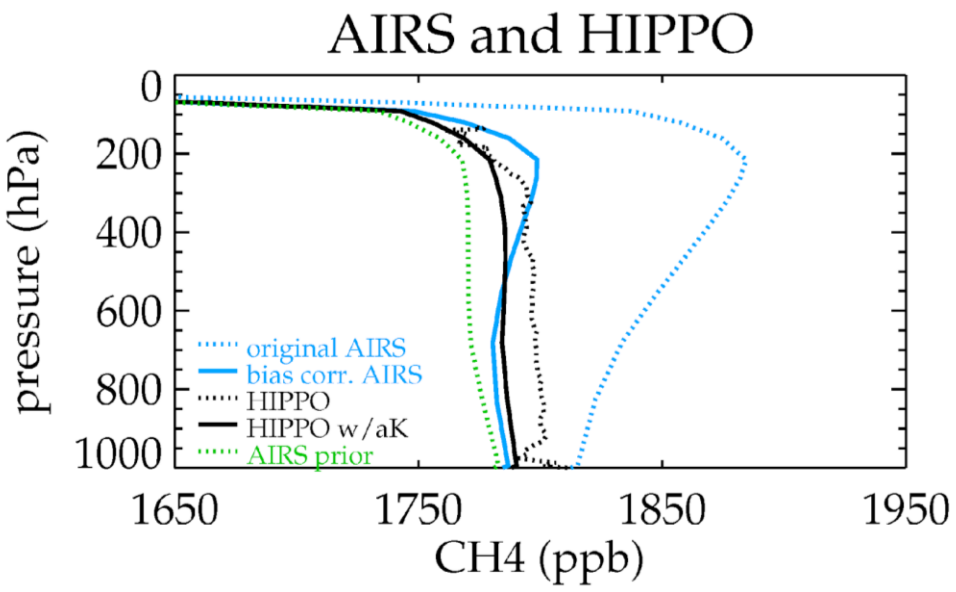

Figure 6: Example of the effect of bias correction on the AIRS profile from averaged HIPPO-1,2,3,5. The blue lines shows the AIRS methane profile before (dotted) and after (solid) bias correction. The black line shows the HIPPO measurements before (dotted) and after averaging kernel is applied (solid).

Formatted: Normal

Formatted: Normal, Space After: 10 pt

Formatted: Font: 9 pt, Bold

Formatted: Font color: Black

Formatted: Normal, Border: Top: (No border), Bottom: (No border), Left: (No border), Right: (No border), Between : (No border), Tab stops: 3.13", Centered + 6.27", Right

~~AIRS versus HIPPO observations (no bias correction)~~

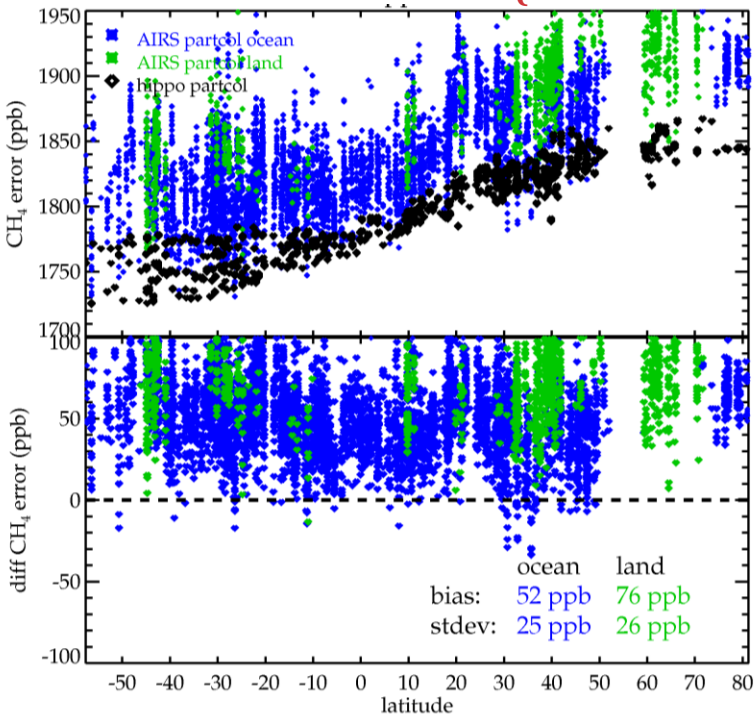

~~Figure 6: Comparison of AIRS methane to aircraft for all HIPPO comparisons over the partial column range measured by the aircraft. Blue shows AIRS ocean observations and green shows AIRS land observations.~~

Formatted: Normal

Formatted: Font color: Black

Formatted: Normal, Border: Top: (No border), Bottom: (No border), Left: (No border), Right: (No border), Between : (No border), Tab stops: 3.13", Centered + 6.27", Right

~~AIRS versus HIPPO observations~~

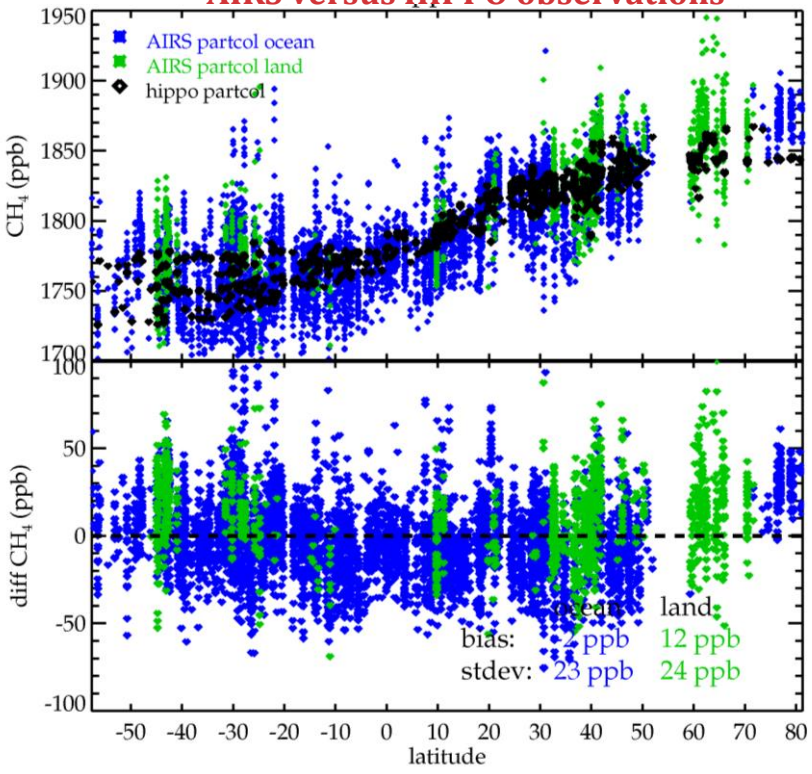

Formatted: Normal

Formatted: Font color: Black

Formatted: Normal, Border: Top: (No border), Bottom: (No border), Left: (No border), Right: (No border), Between : (No border), Tab stops: 3.13", Centered + 6.27", Right

rsus HIPPO observations

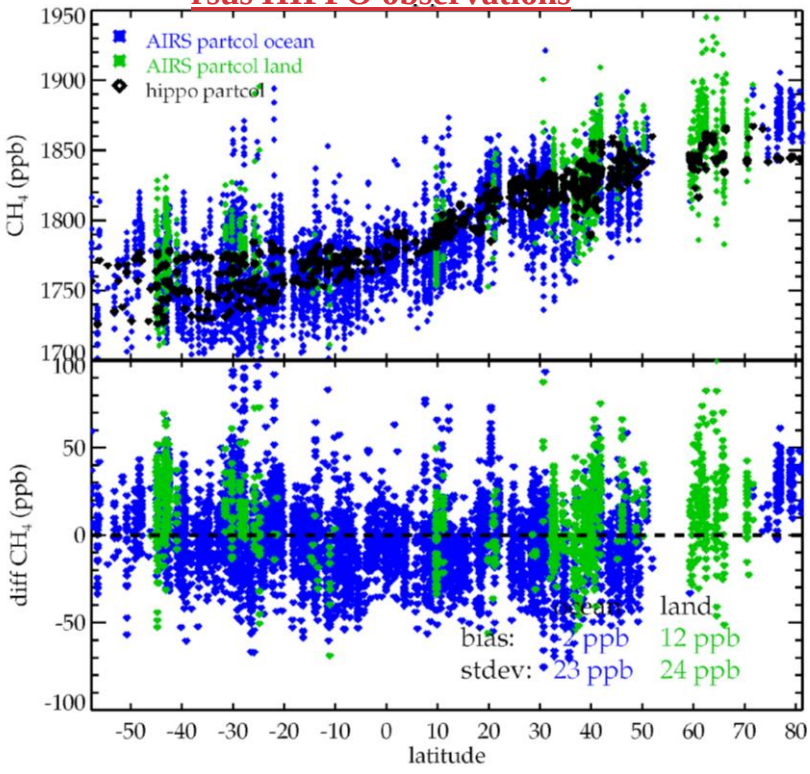

Figure 7: Same as Figure ~~65~~, but after bias correction. The ocean has -2 ppb bias, 23 ppb stdev, and the land has 12 ppb bias, 24 ppb stdev.

Formatted: Normal

Formatted: Font: 9 pt, Bold, Font color: Black

Formatted: Normal, Space After: 10 pt, Border: Top: (No border), Bottom: (No border), Left: (No border), Right: (No border), Between : (No border)

Formatted: Font: 9 pt, Bold, Font color: Black

Formatted: Font color: Black

Formatted: Font color: Black

Formatted: Normal, Border: Top: (No border), Bottom: (No border), Left: (No border), Right: (No border), Between : (No border), Tab stops: 3.13", Centered + 6.27", Right

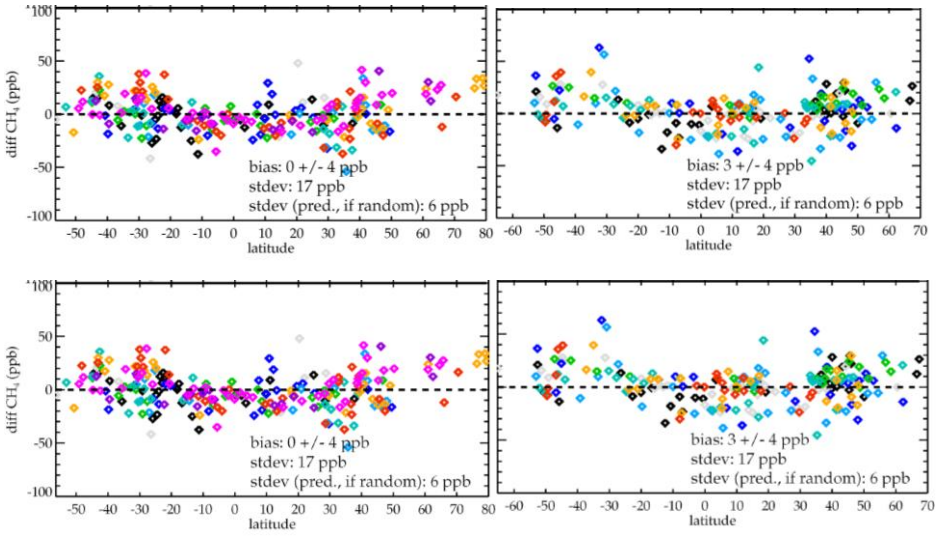

Figure 8: Comparison of daily averaged AIRS to HIPPO measurements (left) and ATom measurements (right) for the partial column observed by the aircraft. The different colors correspond to the campaigns shown in Fig. 1.

Formatted: Normal

Formatted: Font: 9 pt, Bold, Font color: Black

Formatted: Normal, Space After: 10 pt, Border: Top: (No border), Bottom: (No border), Left: (No border), Right: (No border), Between : (No border)

Formatted: Font color: Black

Formatted: Font color: Black

Formatted: Normal, Border: Top: (No border), Bottom: (No border), Left: (No border), Right: (No border), Between : (No border), Tab stops: 3.13", Centered + 6.27", Right

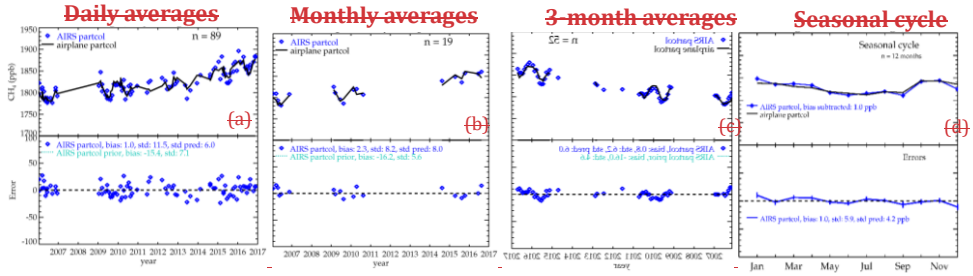

Formatted: Normal

(d)

Formatted: Font color: Black

Formatted: Normal, Border: Top: (No border), Bottom: (No border), Left: (No border), Right: (No border), Between : (No border), Tab stops: 3.13", Centered + 6.27", Right

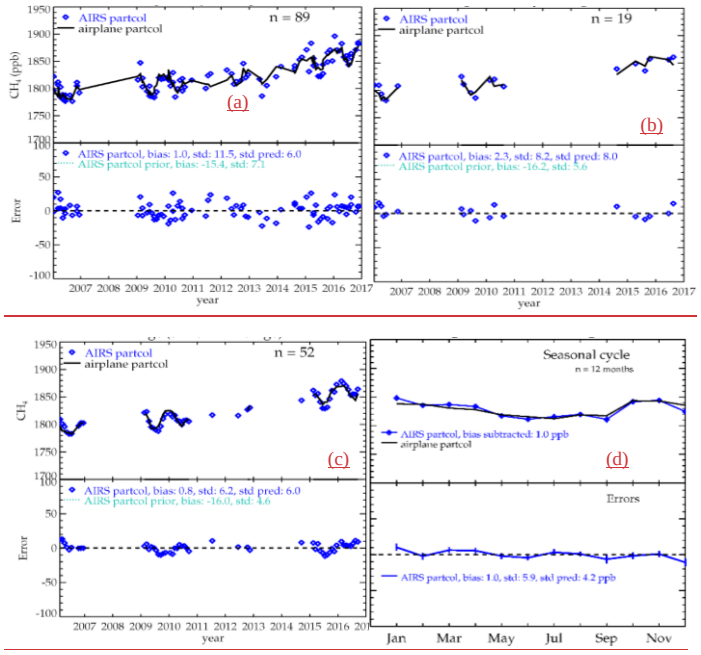

Figure 9: Comparison at TGC (27.7N, 96.9E). (Top) Comparison of AIRS and co-located NOAA aircraft flights in SE Texas for the partial column XCH_4 VMR within the pressure levels measured by the aircraft. Data are averaged over (a) 1 day ~~(a),~~ (b) 1 month ~~(b),~~ (c) 90-days ~~(c),~~ and (d) averaged ~~over~~by month from all years ~~(d).~~ (Bottom) Difference from the aircraft. The predicted error for daily observations is the observation error (27 ppb) divided by the square root of the number of observations. The predicted monthly or seasonal error is the mean daily error (11.5 ppb) divided by the square root of the number of days averaged.

Formatted: Normal

(d)

Formatted: Font: 9 pt, Bold

Formatted: Normal, Space After: 10 pt

Formatted: Font: 9 pt, Bold

Formatted: Font: 9 pt, Bold

Formatted: Font: 9 pt, Bold

Formatted: Font: 9 pt, Bold

Formatted: Font: 9 pt, Bold

Formatted: Font: 9 pt, Bold

Formatted: Font: 9 pt, Bold

Formatted: Font: 9 pt, Bold

Formatted: Font color: Black

Formatted: Normal, Border: Top: (No border), Bottom: (No border), Left: (No border), Right: (No border), Between : (No border), Tab stops: 3.13", Centered + 6.27", Right